4 THERMODYNAMIC CYCLES

Abstract

Energy sources such as coal, natural gas, or petroleum cannot be used directly to perform a work. These sources are burned to generate heat which is then converted to mechanical or electrical energy. These processes are governed by thermodynamic cycles and the efficiency of the overall process depends mainly on the choice or efficiency of the cycle. A number of thermodynamic cycles using various working fluids have been suggested. The description and analysis of these cycles are presented in this chapter.

4.1 Introduction

The energy resources available in nature such as coal, natural gas, petroleum, and uranium cannot be used directly for most of the applications. These resources have to be transformed into a useful form such as heat or electricity before their use. For example, coal must first be burned or combusted to generate heat which is then used to produce steam for space heating or electricity generation. Similarly, crude petroleum must first be refined to obtain gasoline or diesel. In automobiles, gasoline or diesel is first burned to generate heat which is then converted to mechanical energy to move the automobiles. Air is generally used as the carrier of heat. The conversion of heat energy to mechanical or other forms of energy is governed by a series of thermodynamic processes.

A thermodynamic cycle is a series of thermodynamic processes at the end of which the system returns to its initial state. Properties depend only on the thermodynamic state which varies during the operations of the process. During the process, heat is added in certain stages and work is obtained from other stages, but obeys the first law of thermodynamics, which states that the net heat input is equal to the net work output over any cycle. The repeating nature of the process path allows for continuous operation. Thermodynamic cycles are discussed in details in a

T.K. Ghosh and M.A. Prelas, *Energy Resources and Systems: Volume 1: Fundamentals and Non-Renewable Resources*, 89–140.

number of text books [1–9]. Two primary classes of thermodynamic cycles are power cycles and refrigeration cycles. Power cycles are cycles that convert a heat input into a work output, while refrigeration cycles transfer heat from low to high temperatures using work input. In this chapter the emphasis will be on power cycles.

The Carnot cycle is considered an ideal thermodynamic cycle. It is the most efficient cycle possible for converting a given amount of thermal energy into work or, conversely, for using a given amount of work for refrigeration purposes. Any cycle operating between temperatures T_H and T_C, cannot exceed the efficiency of a Carnot cycle. The temperatures are expressed in Kelvin (K) or Rankine (R). Further discussion on Carnot engine efficiency is given by Curzon and Ahlborn [10].

4.2 Carnot Cycle

The Carnot cycle was first studied by Nicolas Léonard Sadi Carnot in the 1820s. Benoit Paul Émile Clapeyron in the 1830s and work in the 1940s further investigated the Carnot cycle.

A Carnot cycle acting as a heat engine is shown in Fig. 4.1 on a temperature (T)-entropy (s) diagram. The cycle takes place between a hot reservoir at temperature T_H and a cold reservoir at temperature T_C. The Carnot cycle consists of the following steps:

Reversible isothermal expansion of the gas at the "hot" temperature, T_H (Isothermal heat addition): During this step (1 to 2 in Fig. 4.1) the expanding gas causes the piston to do work on the surroundings. The gas expansion is propelled by absorption of heat from the high temperature reservoir.

Reversible adiabatic expansion of the gas: For this step (2 to 3 in Fig. 4.1) it is assumed that the piston and cylinder are thermally insulated, so that no heat is gained or lost. The gas continues to expand, doing work on the surroundings. The gas expansion causes it to cool to the "cold" temperature, T_C.

Reversible isothermal compression of the gas at the "cold" temperature, T_C (Isothermal heat rejection): This step is shown as 3–4 in Fig. 4.1. Now the surroundings do work on the gas, causing heat to flow out of the gas to the low temperature reservoir.

Reversible adiabatic compression of the gas: This is Step 4 to 1 in Fig. 4.1. Once again it is assumed that the piston and cylinder are thermally insulated. During this step, the surroundings do work on the gas, compressing it and causing the temperature to rise to T_H. At this point the gas is in the same state as at the start of Step 1.

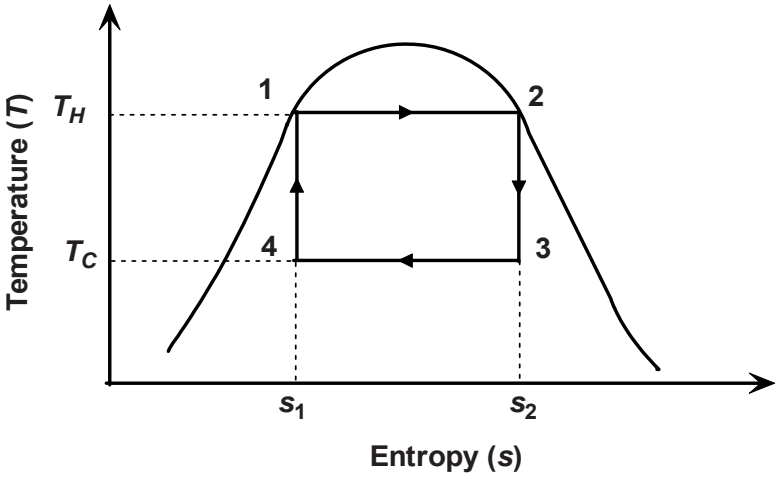

Fig. 4.1. The *T-s* diagram of the Carnot cycle.

4.2.1 Efficiency of Carnot Engine

The amount of energy transferred as work is given by;

$$\Delta W = \int P\,dv = \left(T_H - T_C\right)\left(s_B - s_A\right) \tag{4.1}$$

where W is the work done per unit mass, P is the pressure, v is the specific volume, and s_1 and s_2 are entropies corresponding to State 1 and State 2, respectively. The total amount of thermal energy transferred between the hot reservoir and the system will be:

$$\Delta Q_H = T_H\left(s_B - s_A\right) \tag{4.2}$$

The total amount of thermal energy transferred between the system and the cold reservoir will be:

$$\Delta Q_C = T_C\left(s_B - s_A\right) \tag{4.3}$$

The efficiency η is defined as the amount of work done divided by the heat input to the system from the hot reservoir (T in absolute temperature units, Kelvins):

$$\eta = \frac{\Delta W}{\Delta Q_H} = 1 - \frac{T_C}{T_H} \tag{4.4}$$

For a heat engine, this efficiency represents the fraction of the heat energy extracted from the hot reservoir and converted to mechanical work. For a refrigeration cycle, it is the ratio of energy input to the refrigerator divided by the amount of energy extracted from the hot reservoir.

Example 4.1

An engine is operating based on a Carnot cycle. The temperatures of the hot and cold reservoirs are 200°C and 20°C, respectively. Calculate the thermal efficiency of the cycle. If the work output from the engine is 15 kW, how much heat should be rejected from the condenser?

Solution

The thermal efficiency of the Carnot Cycle is given by

$$\eta = 1 - \frac{T_C}{T_H} = 1 - \frac{20 + 273.15}{200 + 273.15} = 1 - \frac{293.15}{473.15} = 0.38$$

The heat input to the cycle is calculated based on per unit time basis.

$$Q_H = \frac{W}{1 - T_C / T_H} = \frac{15}{0.38} = 39.47 \text{ kW}$$

The heat rejected to the condenser is

$$Q_L = Q_H - W = 39.47 - 15 = 24.47 \text{ kW}$$

In reality it is not possible to build an ideal thermodynamically reversible engine based on the Carnot cycle. Therefore, real heat engines based on real thermodynamic cycles are less efficient than the Carnot cycle. A number of real thermodynamic cycles have been designed based on the process needs. Thermodynamic cycles that are widely used in various day-to-day operations include the following.

(A) Brayton Cycle
   1. Open (gas turbine)
   2. Closed
      (i) Inert working fluid
      (ii) Active working fluid

(B) Otto Cycle (spark ignition)
  1. Reciprocating ("gas" engine)
    (i) 4-stroke cycle
    (ii) 2-stroke cycle
  2. Rotary
  3. Homogeneous Charge Compression Ignition (HCCI)

(C) Diesel Cycle (compression ignition)
  1. Reciprocating
    (i) 4-stroke cycle
    (ii) 2-stroke cycle
  2. Rotary

(D) Dual Cycle

(E) Rankine Cycle
  1. Reheat
  2. Regenerative
    (i) Open feed water
    (ii) Closed feed water
  3. Supercritical

(F) Combined Brayton and Rankine Cycle

(G) Stirling Cycle

(H) Ericsson Cycle

(I) Atkinson Cycle

(J) Miller Cycle

(K) Kalina Cycle

4.3 Brayton Cycle

The Brayton cycle is used for gas turbines only where both the compression and expansion processes take place in rotating machinery. The two major application areas of gas-turbine engines are aircraft propulsion and electric power generation. Gas turbines are used in stationary power plants to generate electricity as stand-alone units or in conjunction with steam power plants on the high-temperature side.

The Brayton cycle may be operated either as an open cycle or as a closed cycle. Gas turbines usually operate on an open cycle, as shown in Fig. 4.2. Fresh air at ambient conditions is drawn into the compressor, where its temperature and pressure are raised. The high-pressure air proceeds into the combustion chamber, where the fuel is burned at constant pressure. The resulting high-temperature gases then enter the turbine, where they expand to the atmospheric pressure through a row of nozzle vanes. This expansion causes the turbine blade to spin, which then turns a shaft inside a magnetic coil. When the shaft is rotating inside the magnetic coil, electrical current is produced. The exhaust gases leaving the turbine in the open cycle are not re-circulated.

The open gas-turbine cycle can be modeled as a closed cycle, as shown in Fig. 4.3, by utilizing the air-standard assumptions. Here the compression and expansion processes remain the same, but a constant-pressure heat-rejection process to the ambient air replaces the combustion process. The working fluid undergoes four internally reversible processes in this closed loop Brayton cycle.

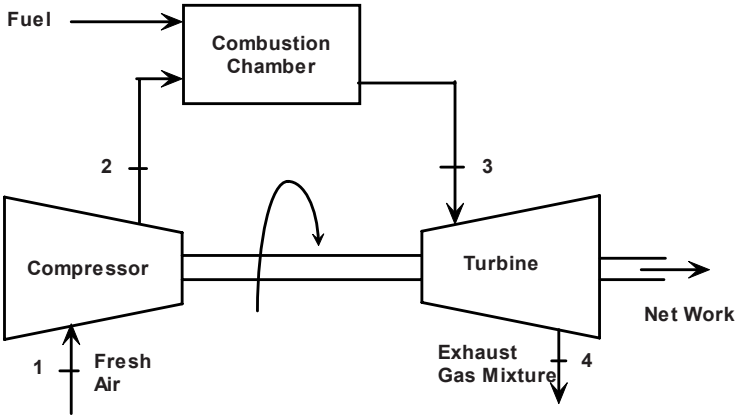

Fig. 4.2. An open cycle gas turbine engine.

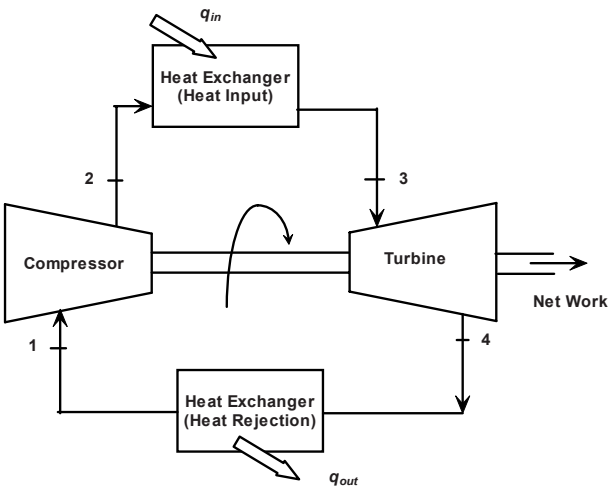

Fig. 4.3. A closed cycle gas turbine engine.

The *P-v* and *T-s* diagrams of an ideal Brayton cycle are shown in Figs. 4.4 and 4.5, respectively. Various stages of the Brayton cycle are as follows:

1–2: Isentropic compression (in a compressor)
2–3: Constant pressure heat addition
3–4: Isentropic expansion (in a turbine)
4–1: Constant pressure heat rejection

However, as shown in Fig. 4.4, during actual operation, the process follows 1–2'–3–4'–1 path.

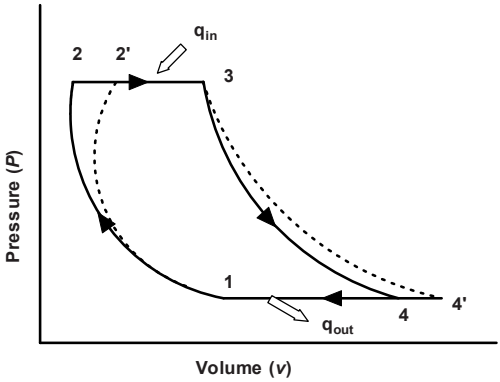

Fig. 4.4. The P-v diagram of the Brayton cycle.

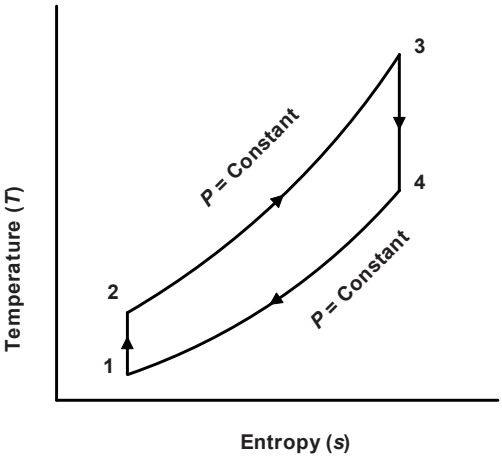

Fig. 4.5. The *T-s* diagram of the Brayton cycle.

The heat balance equation for the system can be written as

$$\left(q_{in} - q_{out}\right) + \left(W_{in} - W_{out}\right) = h_{out} - h_{in} \tag{4.5}$$

where q_{in} is the amount of heat added at the boiler and q_{out} is the amount of heat removed from the condenser (in the case of the closed cycle system) or heat carried away by the exhaust stream (in the case of the open cycle). W_{in} is the work input to the pump and W_{out} is the work output from the turbine. The enthalpy of the stream is given by h. Heat transfers to and from the working fluid can be expressed by:

$$q_{in} = h_3 - h_2 = C_P\left(T_3 - T_2\right) \tag{4.6}$$

$$q_{out} = h_4 - h_1 = C_P\left(T_4 - T_1\right) \tag{4.7}$$

where, C_p is the specific heat at constant pressure and T represents the temperature in Kelvin (K). The thermal efficiency of an ideal Brayton cycle may be expressed as

$$\begin{aligned}
\eta &= \frac{w_{net}}{q_{in}} \\
&= 1 - \frac{q_{out}}{q_{in}} \\
&= 1 - \frac{C_P\left(T_4 - T_1\right)}{C_P\left(T_3 - T_2\right)} \\
&= 1 - \frac{T_1\left(\dfrac{T_4}{T_1} - 1\right)}{T_2\left(\dfrac{T_3}{T_2} - 1\right)}
\end{aligned} \tag{4.8}$$

Processes 1–2 and 3–4 are isentropic. For an adiabatic quasiequilibrium process involving an ideal gas, the following relationships hold:

$$Tv^{k-1} = constant, \quad TP^{\left(\frac{1-k}{k}\right)} = constant, \quad Pv^{k} = constant$$

where, k is the ratio of specific heats ($k = C_p/C_v$). C_p is the specific heat at constant pressure and C_v is the specific heat at constant volume. Since, $P_2 = P_3$, and $P_4 = P_1$, the temperature ratios may be expressed in terms of pressure (P) as:

$$\frac{T_2}{T_1} = \left(\frac{P_2}{P_1}\right)^{\frac{k-1}{k}}$$
$$\frac{T_3}{T_4} = \left(\frac{P_3}{P_4}\right)^{\frac{k-1}{k}} \tag{4.9}$$

From Fig. 4.5,

$$\frac{P_2}{P_1} = \frac{P_3}{P_4} \tag{4.10}$$

This suggests that:

$$\frac{T_4}{T_1} = \frac{T_3}{T_2} \tag{4.11}$$

Using Eqs. (4.9–4.11), the efficiency may be expressed by the following expression.

$$\eta = 1 - \frac{1}{\left(\frac{P_2}{P_1}\right)^{\frac{k-1}{k}}} \tag{4.12}$$

Equation (4.12) suggests that the efficiency of the cycle may be increased by increasing the pressure ratio and the specific heat ratio of the working fluid (if different from air). Various aspects of Brayton cycles have been studied by a number of investigators [11–18]. Applications of Brayton cycles have been explored for a number of new systems, including power plants [19–22], nuclear power plants [23–30], space power applications [31–36], coal gasification plants [37], waste heat recovery system [38], automobile engines [39–42], and using other working fluids [43–50]. Discussion on Brayton cycle efficiency and how it can be improved has been discussed by Sahin et al. [51], Wu et al. [52–56], and Cheng and Chen [57, 58].

Example 4.2

Air enters the compressor of a gas turbine operating on a Brayton Cycle at ambient conditions (100 kPa and 25°C). It leaves the compressor and combustor at 500 kPa and 850°C, respectively. Calculate the temperature at various stages of the cycle and the thermal efficiency.

Solution

The following information is given:

$T_1 = 25 + 273.15 = 298.15$ K, and $T_3 = 850 + 273.15 = 1123.15$ K, $P_1 = 100$ kPa, and $P_2 = 500$ kPa. The value of k for air is 1.4.

From Eq. (4.9),

$$T_2 = T_1\left(\frac{P_2}{P_1}\right)^{\left(\frac{k-1}{k}\right)} = 298.15\,(5)^{0.286} = 472\,\text{K}$$

Similarly,

$$T_4 = T_3\left(\frac{P_4}{P_5}\right)^{\left(\frac{k-1}{k}\right)} = 1123.15\left(\frac{1}{5}\right)^{0.286} = 709.0\,\text{K}$$

The thermal efficiency calculated from Eq. (4.12) is 0.369 or 36.9%

4.4 The Otto Cycle

All internal combustion engines are operated based on the Otto thermodynamic cycle. The process is shown on the P-v diagram in Fig. 4.6.

The movement and location of the piston in the cylinder during the cycle is shown in Fig. 4.7. The diameter of the piston is called the bore and the distance the piston travels in a direction is called the stroke. During the intake stroke, the piston does not travel all the way to the bottom of the cylinder. When the piston moves to the lowest allowable point at the bottom, known as Bottom Dead Center (BDC), the air occupies the maximum volume. Similarly, the piston moves only to a specified distance during the compression stroke. At the end of the compression stroke, the volume occupied by the air in the cylinder is at a minimum and called Top Dead Center (TDC). This volume is the clearance volume.

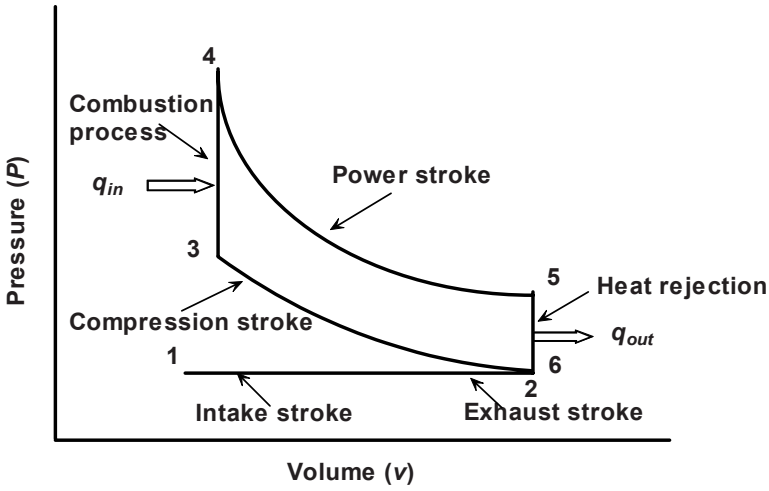

Fig. 4.6. The *P*-*v* diagram of the Otto cycle.

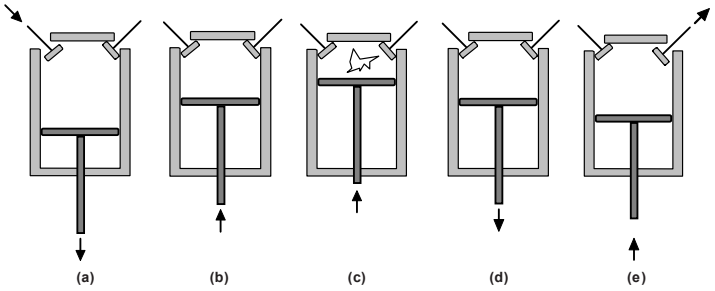

Fig. 4.7. Position of pistons in the cylinder for a 4-stoke Otto engine.

The cycle proceeds as follows:

Stage 1: The intake valve opens and a mixture of fuel and air is drawn into the cylinder. The piston is pulled towards the crankshaft, as shown in Fig. 4.7a, at constant pressure. In the *P*-*v* diagram, 1–2 is Stage 1 and is the beginning of the intake stroke.

Stage 2: At the end of the intake stroke, the intake valve is closed and the piston is moved back towards the combustion chamber (Fig. 4.7b). The pressure and temperature are increased by the adiabatic compression (Step 2–3 in the *P*-*v* diagram). Stage 2 is the beginning of the compression stroke.

Stage 3: At the end of the compression stroke, the spark plug in the engine, which generates an electric spark, ignites the fuel-air mixture (Fig. 4.7c). Stage 3 is the beginning of the combustion process and is Step 3–4 in the *P*-*v* diagram.

Stage 4: This is called the power stroke and is shown in Step 4–5 in the *P*-*v* diagram. Combustion occurs very quickly at constant volume in the combustion chamber in an Internal Combustion (IC) engine. The high pressure forces the piston back towards the crankshaft as shown in Fig. 4.7d.

Stage 5: This is the end of the power stroke, and heat is rejected to the surroundings as shown in Step 5–6 in the *P*-*v* diagram.

Stage 6: Following heat rejection, the exhaust valve is opened and the residual gas is forced out into the surroundings to prepare for the next intake stroke (Fig. 4.7e). Stage 6 is the beginning of the exhaust stroke.

Work is done on the gas by the piston between Stages 2 and 3. Work is done by the gas on the piston between Stages 4 and 5. Therefore, the area enclosed by the cycle on a *P*-*v* diagram is proportional to the work produced by the cycle. The work times the rate of the cycle (cycles per second) is equal to the power produced by the engine. For calculation of the efficiency of an Otto cycle, first an ideal cycle should be considered in which there is no heat entering (or leaving) the gas during the compression and power strokes, no friction losses, and instantaneous burning occurring at constant volume. In actual operation, there are many losses associated with each process. These losses are taken into account by introducing efficiency factors. The ideal efficiency of the cycle may be calculated using the following simplified *P*-*v* diagram (Fig. 4.8).

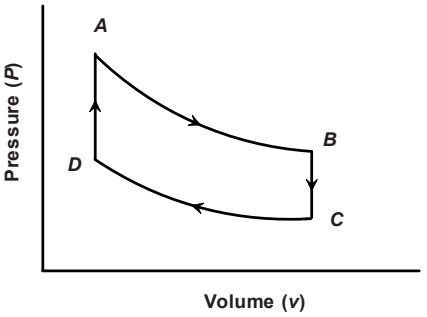

Fig. 4.8. A simplified *P*-*v* diagram of the Otto cycle.

The work done by the air-standard Otto cycle may be determined by a total energy balance.

$$W = q_{DA}\left(\frac{q_{DA} + q_{BC}}{q_{DA}}\right) \tag{4.13}$$

The heat input or rejection may be described in terms of temperature as follows.

$$\begin{aligned} q_{DA} &= C_v\left(T_A - T_D\right) \\ q_{BC} &= C_v\left(T_C - T_B\right) \end{aligned} \tag{4.14}$$

where *Cv* is the heat capacity at constant volume. The efficiency, therefore, can be expressed as

$$\eta = \frac{W}{q_{DA}} = \frac{C_v\left(T_A - T_D\right) - C_v\left(T_B - T_C\right)}{C_v\left(T_A - T_D\right)} \tag{4.15}$$

$$\eta = 1 - \frac{T_B - T_C}{T_A - T_D} \tag{4.16}$$

As mentioned earlier, for the adiabatic reversible processes, the following relationship holds for air as it can be assumed to behave as an ideal gas

$$Pv^k = cons\tan t \tag{4.17}$$

Using this relationship, the temperature at various point of the cycle can be expressed as follows.

$$\begin{aligned} T_B &= \frac{P_B v_B}{R} = \frac{P_B v_C}{R} \\ T_C &= \frac{P_C v_C}{R} \\ T_A &= \frac{P_A v_A}{R} = \frac{P_A v_D}{R} \\ T_D &= \frac{P_D v_D}{R} \end{aligned} \tag{4.18}$$

Therefore,

$$\begin{aligned} P_A v_D^k &= P_B v_C^k \\ P_C v_C^k &= P_D v_D^k \end{aligned} \tag{4.19}$$

By defining the compression ratio as the ratio of the volume occupied by the air at BDC to the volume occupied by air at TDC, the following expression is obtained.

$$r = \frac{v_C}{v_D} \tag{4.20}$$

The efficiency for the cycle can be written as

$$\eta = 1 - \left(\frac{1}{r}\right)^{\gamma - 1} \tag{4.21}$$

The work W can be expressed by the temperatures as follows

$$W = C_v\left[\left(T_4 - T_3\right) - \left(T_5 - T_2\right)\right] \tag{4.22}$$

The work times the rate of the cycle (cycles per second, *cps*) is equal to the power produced by the engine.

$$Power = W \bullet cps \tag{4.23}$$

The mean effective pressure (MEP) is another quantity that can be used to rate piston-cylinder engines and is given by the following expression.

$$W_{cycle} = \left(MEP\right)\left(v_{BDC} - v_{TDC}\right) \tag{4.24}$$

As noted by Mandl [59], for a car with $r = 10$, the theoretical expression gives an efficiency of 0.6, but the practical efficiency is more like 0.3. A table of thermal efficiencies and peak cylinder pressure and combustion temperature is given by Anderson [60]. Thermodynamic analysis of the Otto cycle has been performed by a number of investigators using first and second law analysis method [61–73]. An attempt has also been made to use the Otto cycle for solar collectors [74].

4.5 Diesel Cycle

In diesel engines, the fuel and air are compressed separately and brought together at the time of combustion. In this arrangement, fuel is injected into the cylinder which contains compressed air at a higher temperature than the self-ignition temperature of the fuel. Once injected, the fuel ignites on its own and does not need an ignition system. It should be noted that the upper limit of compression ratio is limited in spark ignition engines due to the self-ignition temperature of the fuel. Therefore, diesel engines are not limited by the fuel to air compression ratio.

The diesel cycle is similar to the Otto cycle; the main difference is in the process of heat addition. In the diesel cycle, the heat addition takes place at constant pressure whereas in the Otto cycle it is at a constant volume. For this reason, the diesel cycle is often referred to as the constant-pressure cycle. The *P*-*v* and *T*-*s* diagrams of the diesel cycle are shown in Figs. 4.9 and 4.10, respectively.

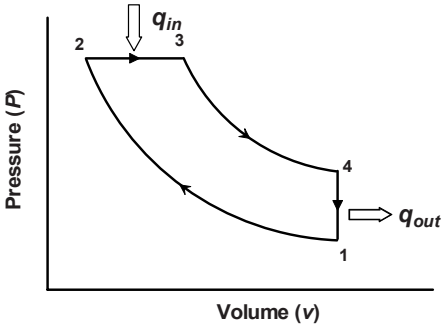

Fig. 4.9. The *P*-*v* diagram of the diesel cycle.

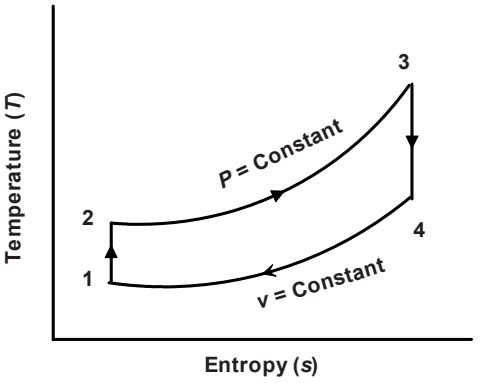

Fig. 4.10. The *T*-*s* diagram of the diesel cycle.

The diesel cycle is an ideal air standard cycle consisting of the following four processes:

1–2: Isentropic compression
2–3: Reversible constant pressure heating
3–4: Isentropic expansion
4–1: Reversible constant volume cooling

The maximum theoretical efficiency of a diesel engine can be calculated in the same way as described earlier for Carnot or Brayton cycles. The efficiency of the diesel cycle can be expressed as:

$$\eta = 1 - \frac{1}{k}\frac{r_e^k - 1}{r_c^{k-1}(r_e - 1)} \tag{4.25}$$

where k is the ratio of the specific heats. The expansion ratio (r_e) and compression ratio (r_c) are given by the following expressions.

$$r_e = \frac{v_3}{v_2} \tag{4.26}$$

$$r_c = \frac{v_1}{v_2} \tag{4.27}$$

The performance of a diesel engine under various conditions has been investigated by several researchers [75–79]. One of the main concerns of diesel engines is emission of pollutants. Several approaches including direct water injection have been explored for reduction of pollutants from a diesel engine [80–82].

Example 4.3

A diesel cycle operates on air with a pressure of 200 kPa and 200°C. The compression ratio is 15. If 1,000 kJ/kg of work output is desired, determine the thermal efficiency of the cycle. What is the MEP for the cycle? What will be the efficiency of an Otto cycle under similar operating conditions?

Solution

Determine the compression ratio, r_c. Assume ideal gas law:

$$v_1 = \frac{RT_1}{P_1} = \frac{(0.287)(200 + 273)}{200} = 0.6788 \text{ m}^3/\text{kg}$$

The compression ratio, r_c, is given by

$$r_c = \frac{v_1}{v_2} = 15 \text{, therefore, } v_2 = 0.6788/15 = 0.04525 \text{ m}^3/\text{kg}$$

Since process 1 to 2 is isentropic, it can be shown that

$$T_2 = T_1\left(\frac{v_1}{v_2}\right)^{k-1} = (200+273)(15)^{0.4} = 1397.3 \text{ K}$$

In terms of pressure, the relationship is given by,

$$P_2 = P_1\left(\frac{v_1}{v_2}\right)^{k} = 200(15)^{1.4} = 8862.5 \text{ kPa}$$

The net work done by the cycle can be calculated as

$$w_{net} = q_{net} = q_{2-3} + q_{4-1} = C_p(T_3 - T_2) + C_v(T_1 - T_4)$$

Substituting the values for *Wnet*, C_p, C_v, T_1, and T_2, we get

$$1000 = 1.00(T_3 - 1397.3) + 0.717(473 - T_4)$$

T_3 and T_4 are unknown, but can be expressed in terms of v_3 by using the following expressions.

$$T_3 = v_3\frac{T_2}{v_2} = 30879.5\,v_3$$

$$T_4 = T_3\left(\frac{v_3}{v_4}\right)^{k-1} = T_3\left(\frac{v_3}{0.6788}\right)^{0.4} = 1.1676\,T_3 v_3^{0.4} = 36054.97\,v_3^{1.4}$$

It may be noted that $v_4 = v_1$. Substitution of T_4 and T_3 provides the following expression

$$1000 = (30879.5\,v_3 - 1397.3) + 0.717(473 - 36054.97 v_3^{1.4})$$

This equation must be solved by a trial and error method. The solution provides the following values:

$v_3 = 0.1$ m^3/kg, $T_3 = 3087.95$ K, and $T_4 = 1435.4$ K.

The cut off ratio r_e is given by

$$r_e = \frac{v_3}{v_2} = \frac{0.1}{0.04525} = 2.21$$

The thermal efficiency is given by Eq. (4.13) and is 0.60 or 60%. The MEP can be calculated as follows.

$$MEP = \frac{W_{net}}{v_1 - v_2} = \frac{1000}{0.6788 - 0.04525} = 1578.4\,\text{kPa}$$

Under similar conditions, the efficiency of an Otto cycle can be calculated from Eq. (4.27). However, the compression ratio, r_c, of Otto cycle is given by

$$r_{c,Otto} = \frac{v_1}{v_3} = \frac{0.6788}{0.1} = 6.788$$

$$\eta_{Otto} = 1 - \left(\frac{1}{r_{Otto}}\right)^{k-1} = 1 - \left(\frac{1}{6.788}\right)^{0.4} = 0.5351 \text{ or } 53.51\%.$$

4.6 The Dual Cycle

A dual cycle approximates an ideal cycle better during the actual performance of a compression-ignition engine. In this cycle, the combustion process is modeled by two heat-addition processes: a constant volume process and a constant pressure process. The process is shown in Fig. 4.11.

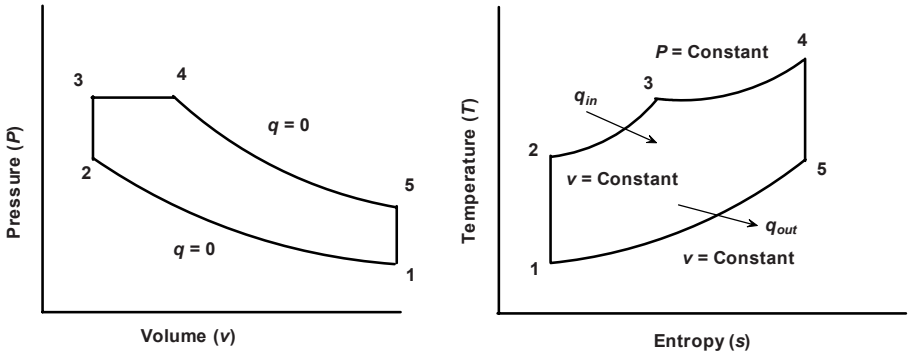

Fig. 4.11. The *P*-*v* and *T*-*s* diagrams of the dual cycle.

The thermal efficiency in terms of temperature can be expressed by the following expression:

$$\eta = 1 - \frac{T_5 - T_1}{T_3 - T_2 + k(T_4 - T_3)} \tag{4.28}$$

In terms of pressure, the thermal efficiency may be expressed as

$$\eta = 1 - \left(\frac{1}{r^{k-1}}\right)\left(\frac{r_p r_c^k - 1}{k r_P (r_c - 1) + r_P - 1}\right) \tag{4.29}$$

where, $r_P = \dfrac{P_3}{P_2}$. (4.30)

The effect of working fluid on dual cycle efficiency has been studied by Chen et al. [83] and Zheng et al. [84]. Dual cycles have been developed for a variety of applications including its use in gas turbines [85], coal gasification units [86], and boiling water reactors for power generation using nuclear energy [87, 88].

4.7 Rankine Cycle

Rankine cycles describe the operation of steam turbines used in power generation plants [89–93]. This is also known as the vapor power cycle as the working fluid changes phase from a liquid to a vapor within the system. A schematic of a Rankine cycle is shown in Fig. 4.12 and the *T-s* diagram of the process is shown in Fig. 4.13. There are four processes or steps in the Rankine cycle. These states are identified by number in the diagram below.

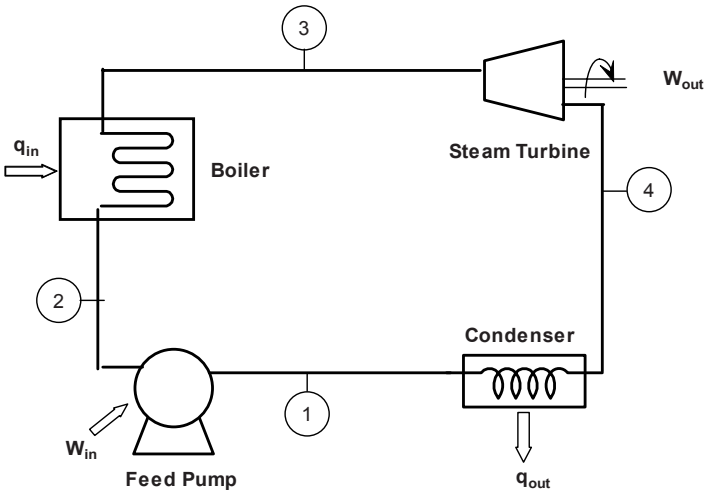

Fig. 4.12. The schematic of the Rankine cycle.

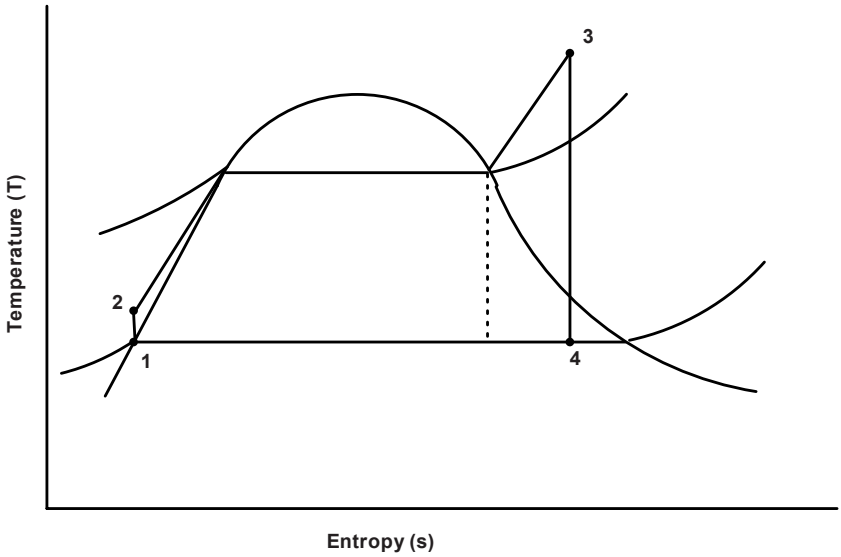

Fig. 4.13. The *T-s* diagram of the Rankine cycle.

Process 1–2: The working fluid is pumped or pressurized isentropically from low to high pressure by a pump. Pumping requires a power input (for example mechanical or electrical).

Process 2–3: The high pressure liquid enters a boiler where it is heated at constant pressure to saturated vapor. Heat sources for power plant systems could be coal, natural gas, or nuclear power.

Process 3–4: The saturated vapor expands through a turbine to generate power output. Ideally, this expansion is isentropic. This decreases the temperature and pressure of the vapor.

Process 4–1: The vapor then enters a condenser where it is cooled to saturated liquid. This liquid then re-enters the pump and the cycle repeats.

In a real Rankine cycle, the compression by the pump and the expansion in the turbine are not isentropic. This increases the power required by the pump and decreases the power generated by the turbine. It also makes calculations more involved and difficult.

Work output of the cycle (Steam turbine), $W_{out,}$ and work input to the cycle (Pump), W_{in}, are given by:

$$W_{out} = \dot{m}\left(h_3 - h_4\right) \tag{4.31}$$

$$W_{in} = v_1(P_2 - P_1) \tag{4.32}$$

where $\dot{m}$ is the mass flow of the cycle. Heat supplied to the cycle (boiler), q_{in} and heat rejected from the cycle (condenser), q_{out} are:

$$q_{in} = \dot{m}(h_3 - h_2) \tag{4.33}$$

$$q_{out} = \dot{m}(h_4 - h_1) \tag{4.34}$$

The net work output of the cycle is:

$$W = W_{out} - W_{in}$$

The thermal efficiency of a Rankine cycle is:

$$\eta = \frac{W}{q_{in}} = \frac{W_{out} - W_{in}}{q_{in}} \approx \frac{W_{out}}{q_{in}} \text{ , since } W_{in} << W_{out} \tag{4.35}$$

The efficiency of the Rankine cycle is not as high as the Carnot cycle but the cycle has less practical difficulties and is more economical. Two main variations of the basic Rankine cycle are used in modern practice.

4.7.1 Rankine Cycle With Reheat

One of the major issues with a Rankine cycle with a high boiler pressure or a low condenser pressure is the formation of liquid droplets in the low pressure side of the turbine. The reheat cycle is often used to prevent liquid droplet formation. The first turbine accepts vapor from the boiler at high pressure. After the vapor has passed through the first turbine, it re-enters the boiler and is reheated before passing through a second, lower pressure turbine. Among other advantages, this prevents the vapor from condensing during its expansion which can seriously damage the turbine blades. The reheat cycle does not significantly influence the thermal efficiency of the cycle, but it does increase the work out. The reheat cycle requires additional investment for equipment and also increases the maintenance costs. An economic analysis should be preformed to justify the reheat cycle. A schematic diagram of the reheat Rankine cycle is given in Fig. 4.14 and various thermodynamic states are given in Fig. 4.15.

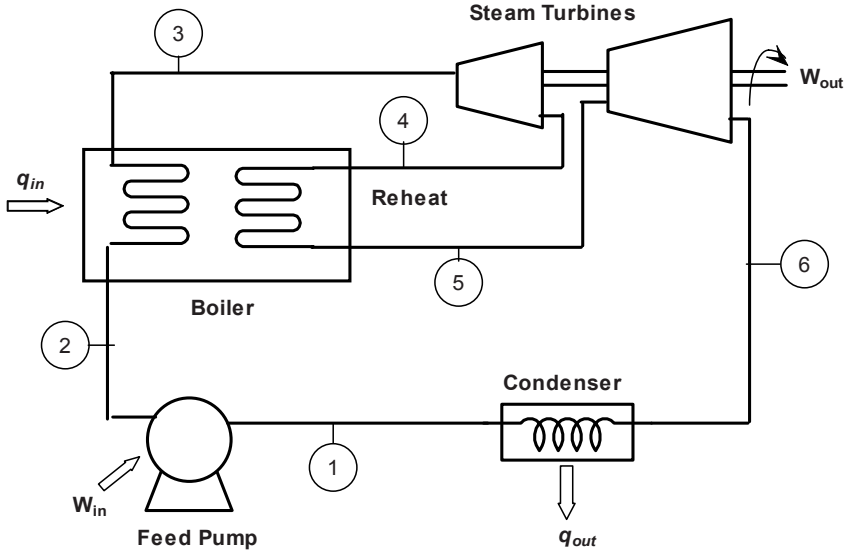

Fig. 4.14. Schematic of a reheat Rankine cycle.

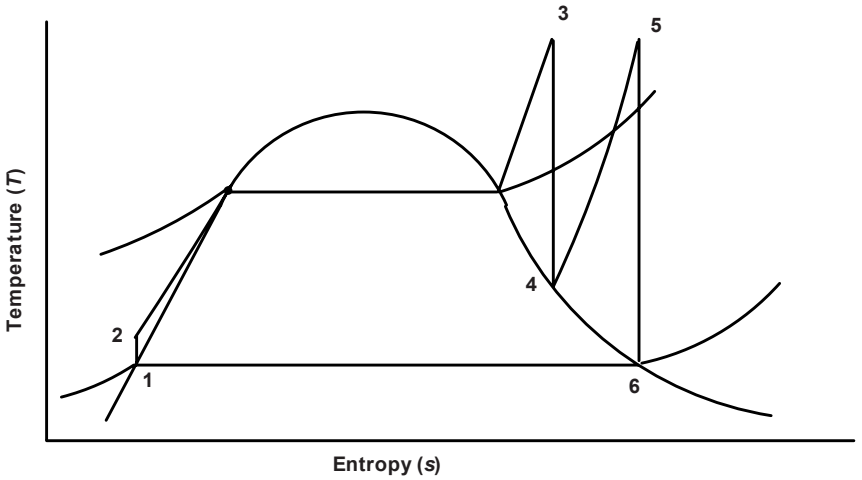

Fig. 4.15. The *T-s* diagram of a reheat Rankine cycle.

The total heat input to the cycle is given by

$$q_{in} = q_{primary} + q_{reheat} = (h_5 - h_4) + (h_3 - h_2) \tag{4.36}$$

The total work output is the combination of the work output from both the turbines and is given by

$$W_{out} = W_{turbine1} + W_{turbine2} = (h_5 - h_6) + (h_3 - h_4) \tag{4.37}$$

The thermal efficiency is expressed as

$$\eta = \frac{W_{out}}{q_{in}} \tag{4.38}$$

4.7.2 Regenerative Rankine Cycle

In the regenerative Rankine cycle, the working fluid, water, after emerging from the condenser possibly as a subcooled liquid is heated by steam tapped from the hot portion of the cycle. This can reduce the energy required to heat the high pressure water to its saturation temperature in the boiler. This would avoid the necessity of condensing all of the steam. A cycle which utilizes this type of reheating is called a regenerative cycle and a schematic diagram of the major elements of the cycle is shown in Fig. 4.16. The *T-s* diagram of such a cycle is shown in Fig. 4.17.

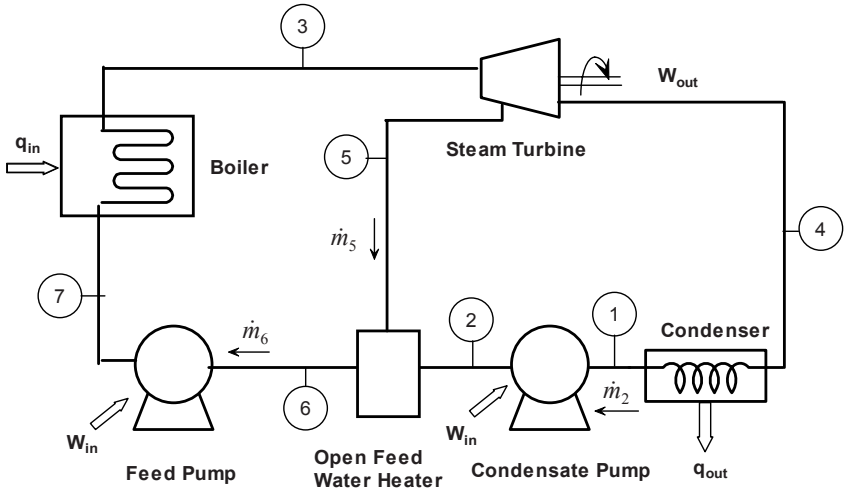

Fig. 4.16. Schematic of a regenerative Rankine cycle with an open feed water heater.

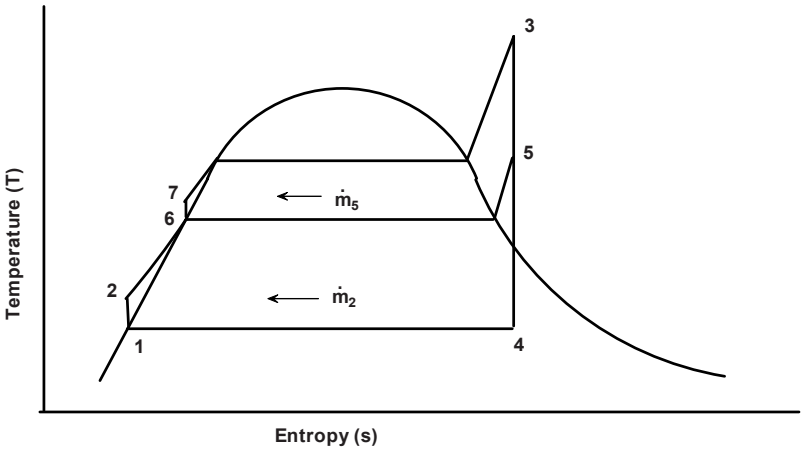

Fig. 4.17. The T-s diagram of the regenerative Rankine cycle.

The water entering the boiler is generally referred to as feedwater and the device used to mix the extracted steam and the condenser water is called a feedwater heater. Two types of schematics can be used for the feedwater heater:

- Open feedwater heater: In this scheme, condensate is mixed directly with the steam in a mixing chamber.
- Closed feedwater heater: In this arrangement, mixing of the two streams is not allowed. The feedwater heater rather is a heat exchanger in which water passes through tubes and the steam condenses on the outer surface of the tubes.

Analysis of a Rankine cycle with an open feedwater heater requires a mass balance of the control volume surrounding the feedwater heater. The mass balance equation is given by,

$$\dot{m}_6 = \dot{m}_5 + \dot{m}_2 \tag{4.39}$$

An energy balance equation assuming no heat loss can be written as

$$\dot{m}_6 h_6 = \dot{m}_5 h_5 + \dot{m}_2 h_2 \tag{4.40}$$

Therefore, the mass input to the feedwater pump is given by

$$\dot{m}_6 = \frac{(h_5 - h_2)}{(h_6 - h_2)} \dot{m}_5 \tag{4.41}$$

If it is assumed that $\dot{m}_6 = 1$, then the total heat input to the cycle is given by;

$$q_{in} = h_3 - h_7 \tag{4.42}$$

and, work output from the turbine is given by;

$$W_{out} = h_3 - h_5 + \dot{m}_2 \left(h_5 - h_4 \right) \tag{4.43}$$

Therefore, the efficiency can be expressed by;

$$\eta = \frac{W_{out}}{q_{in}} = \frac{h_3 - h_5 + \dot{m}_2 \left(h_5 - h_4 \right)}{\left(h_3 - h_7 \right)} \tag{4.44}$$

The schematic of the regenerative Rankine cycle with a closed feed water heater is explained in Fig. 4.18. In this configuration, part of the stream from the turbine is mixed directly with that from the condenser. In general, the more feed-water heaters, the better is the cycle efficiency.

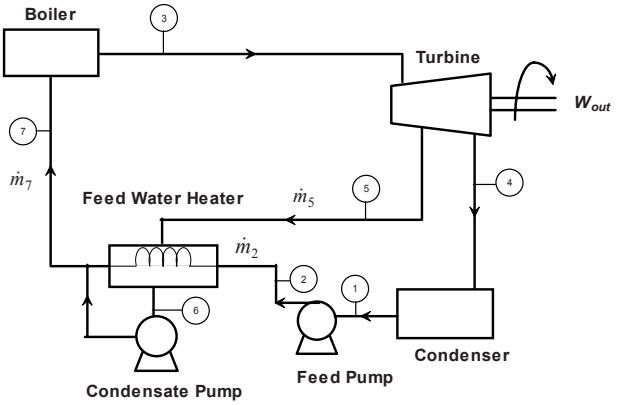

Fig. 4.18. Schematic of a regenerative Rankine cycle with a closed feed water heater.

4.8 Supercritical Rankine Cycle

New materials are allowing the use of much higher temperature in power plants [94, 95]. As discussed in Chapter 6, a number of supercritical power plants are now in operations world wide, which use a supercritical Rankine cycle [96–105]. A pressure of 30 MPa and a temperature greater than 600^{o}C are generally used in supercritical power plants. The *T*-*s* diagram of the cycle is shown in Fig. 4.19.

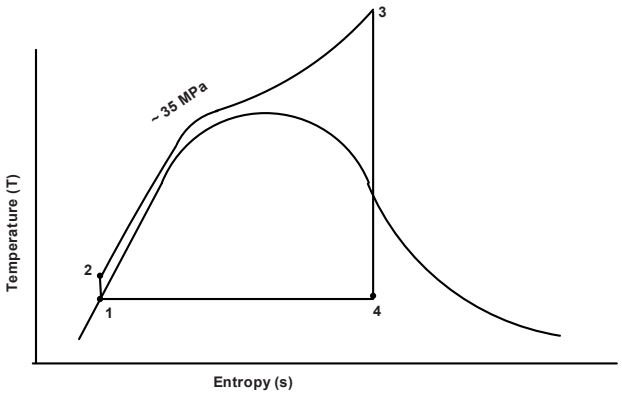

Fig. 4.19. The *T-s* diagram of a Rankine cycle operating under supercritical condition of steam.

4.9 Combined Reheat and Regenerative Rankine Cycle

The regenerative cycle generally has problems with water droplets at the low pressure side of the turbines. To overcome this problem, several power plants combine a reheat cycle with a regenerative cycle. This increases the thermal efficiency. A typical combined cycle is shown in Fig. 4.20 and the *T-s* diagram of the process is shown in Fig. 4.21.

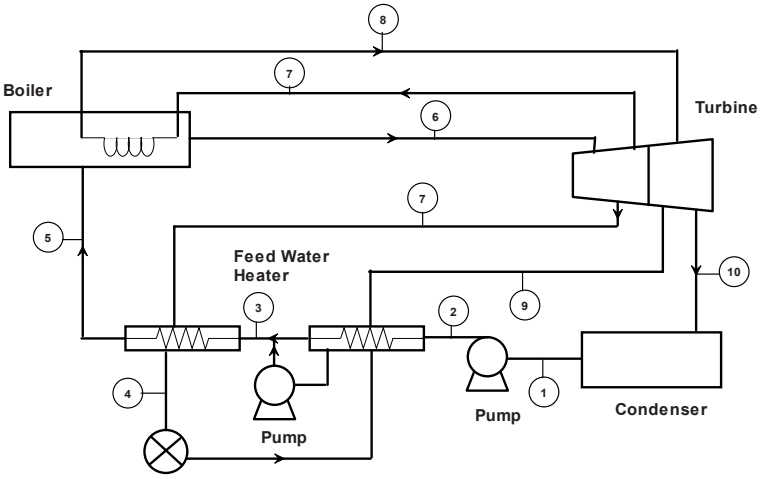

Fig. 4.20. Schematic of a reheat-regenerative Rankine cycle Numbers in the figure refer to various thermodynamic states that are shown in the *T-s* diagram below.

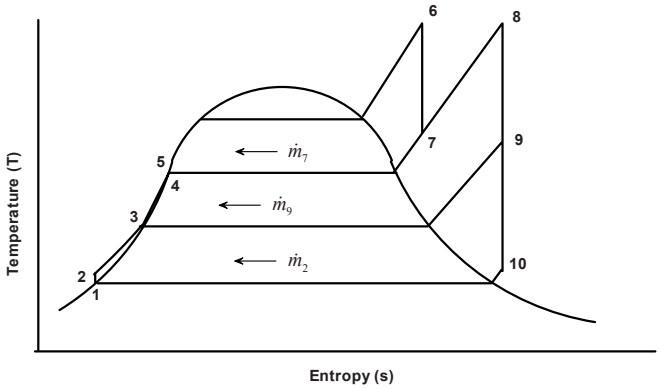

Fig. 4.21. The *T-s* diagram of a reheat-regenerative Rankine cycle.

Example 4.4

A supercritical Rankine cycle operates between pressures of 30 MPa and 10 kPa with a maximum temperature of 600°C. The cycle contains two reheat stages and two open feedwater heaters. The high pressure turbine operates between 30 MPa and 4 MPa. A portion of the steam is reheated to 600°C and expanded in another turbine to 200 kPa. A portion of the extracted steam is again reheated to 350°C and finally expanded to 10 kPa in the final low pressure turbine. Show the cycle in a *T-s* diagram and calculate the efficiency of the cycle.

Solution

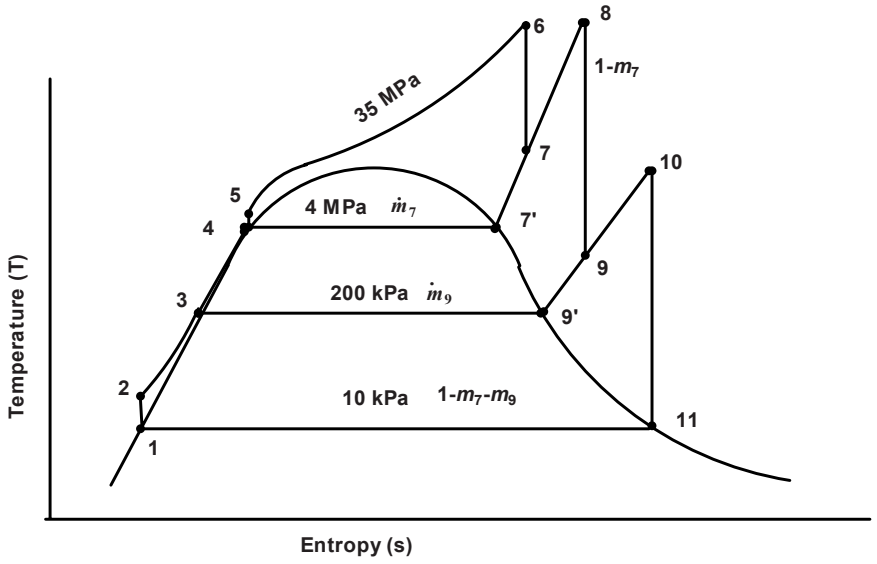

Using a steam table (Appendix IV), the following values for enthalpy, and entropy are obtained. The condition of the steam is noted in the parenthesis.

h_1 (Saturated water at 10 kPa) = h_2 = 191.8 kJ/kg
h_3 (Saturated water at 200 kPa) = 504.7 kJ/kg
h_4 (Saturated water at 4 MPa) = h_5 = 1087.3 kJ/kg
h_6 (Superheated steam at 30 MPa, 600°C) = 3443.9 kJ/kg
h_8 (Superheated steam at 4 MPa, 600°C) = 3674.4 kJ/kg
h_{10} (Superheated steam at 200 kPa, 350°C) = 3174.3 kJ/kg
$s_6 = s_7$ = 6.2331 kJ/kg.K; $s_8 = s_9$ = 7.3696 kJ/kg.K; $s_{10} = s_{11}$ = 8.0636 kJ/kg.K

The values of h_7 and h_9 are determined by interpolation as follows.

To find, h_7, the data is interpolated between stage 6 and saturated stage 7'. Similarly, h_9 was found by interpolation between stage 8 and saturated stage 9'.

$$h_7 = \left(\frac{6.2339 - 6.0709}{6.3622 - 6.0709}\right)(2961 - 2801) + 2801 = 2891\,\text{kJ/kg}$$

$$h_9 = \left(\frac{7.3696 - 7.2803}{7.5074 - 7.2803}\right)(2870 - 2769) + 2769 = 2809\,\text{kJ/kg}$$

The fraction of the steam at stage 11, is calculated as follows.

$$x_{11} = \frac{8.0636 - 0.6491}{7.5019} = 0.9883$$

$$h_{11} = 191.8 + (0.9883)(2393) = 2557\,\text{kJ/kg}$$

The mass flow rates in the high and low pressure heaters are calculated as follows.

$$h_5 = h_7\dot{m}_7 + (1 - \dot{m}_7)h_3,\ \dot{m}_7 = \frac{h_5 - h_3}{h_7 - h_3} = 0.2439\,\text{kg/s}$$

$$(1 - \dot{m}_7)h_3 = \dot{m}_9 h_9 + (1 - \dot{m}_7 - \dot{m}_9)h_2,\ \dot{m}_9 = \frac{(1 - \dot{m}_7)h_3 - h_2 - \dot{m}_7 h_2}{h_9 - h_2}$$

Substituting values, $\dot{m}_9 = 0.0904$ kg/s

The power from the turbine is given by

$$\dot{W}_T = 1(h_6 - h_7) + (1 - \dot{m}_7)(h_8 - h_9) + (1 - \dot{m}_7 - \dot{m}_9)(h_{10} - h_{11})$$

Or,

$$\begin{aligned}\dot{W}_T &= (3444 - 2891) + (1 - 0.2439)(3674 - 2809) + \\ &\quad (1 - 0.2439 - 0.0904)(3174 - 2557) \\ &= 1,609 \text{ KW}\end{aligned}$$

The energy input to the boiler is given by

$$\begin{aligned}q_{in} &= 1(h_6 - h_5) + (1 - \dot{m}_7)(h_8 - h_7) + (1 - \dot{m}_7 - \dot{m}_9)(h_{10} - h_9) \\ &= (3444 - 1087) + (1 - 0.2439)(3674 - 2891) + \\ &\quad (1 - 0.2439 - 0.0904)(3174 - 2809) \\ &= 3,192\text{KW}\end{aligned}$$

The efficiency of the cycle is

$$\eta = \frac{1609}{3192} = 0.504 \text{ , or } 50.4\%$$

4.10 Combined Cycles in Stationary Gas Turbine for Power Production

The gas temperature at the inlet point of a gas turbine operating in a Brayton cycle is considerably higher than the peak steam temperature used in the steam turbine. Depending on the compression ratio of the gas turbine, the exhaust temperature from the gas turbine could be high enough to permit economic generation of steam and run a steam turbine. A configuration such as this is known as the combined Brayton-Rankine cycle. The schematic of such a combined cycle is shown in Fig. 4.22, and the *T-s* diagram of the cycle is illustrated in Fig. 4.23.

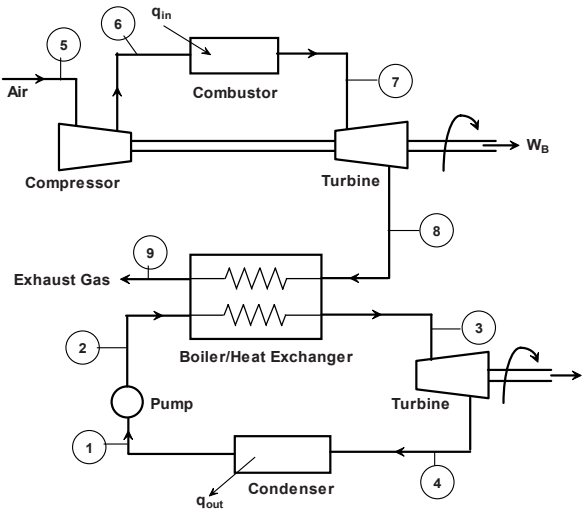

Fig. 4.22. Gas turbine-steam combined cycle.

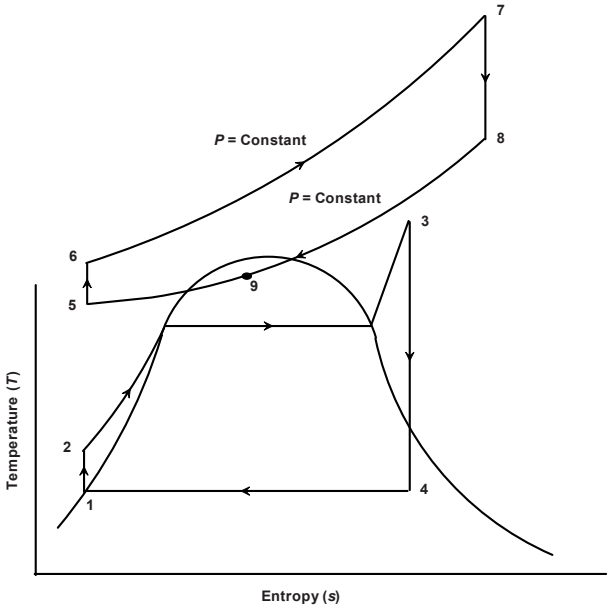

Fig. 4.23. The *T-s* diagram of the combined cycle.

A thermal efficiency analysis of the combined cycle can be carried out as follows. The heat input to the gas turbine can be designated as q_{in}, and the heat rejected to the atmosphere as q_{out}. The heat out of the gas turbine is denoted as q_{GT}. If it is assumed that the heat exchanger is 100% efficient, then the heat input to the Rankine cycle can be denoted as q_{GT} too. The overall combined cycle efficiency can be expressed as

$$\eta_{cc} = \frac{W_{out,Total}}{q_{in}} = \frac{W_B + W_R}{q_{in}} \tag{4.45}$$

where η_{cc} is the overall efficiency of the combined cycle, W_B is the work done by the Brayton cycle and W_R is the work done by the Rankine cycle. Eq. (4.45) can be rearranged as follows:

$$\eta_{cc} = \frac{(q_{in} - q_{GT}) + (q_{GT} - q_{out})}{q_{in}} = \left(1 - \frac{q_{GT}}{q_{in}}\right) + \left(1 - \frac{q_{out}}{q_{GT}}\right)\left(\frac{q_{GT}}{q_{in}}\right) \tag{4.46}$$

The efficiencies of a Brayton cycle and a Rankine cycle can be expressed as follows:

$$\begin{aligned} \eta_B &= 1 - \frac{q_{GT}}{q_{in}} \\ \eta_R &= 1 - \frac{q_{out}}{q_{GT}} \end{aligned} \tag{4.47}$$

Therefore, the combined cycle efficiency becomes

$$\eta_{cc} = \eta_B + \eta_R - \eta_B \eta_R \tag{4.48}$$

The efficiency of a gas turbine cycle is generally on the order of 40%. If we assume that the Rankine cycle efficiency for the combined system will be in the order of 30%, the combined cycle efficiency would be 58%, which is a very large increase over either of the two simple cycles. Some representative efficiencies and power outputs for different cycles are shown in Fig. 4.24.

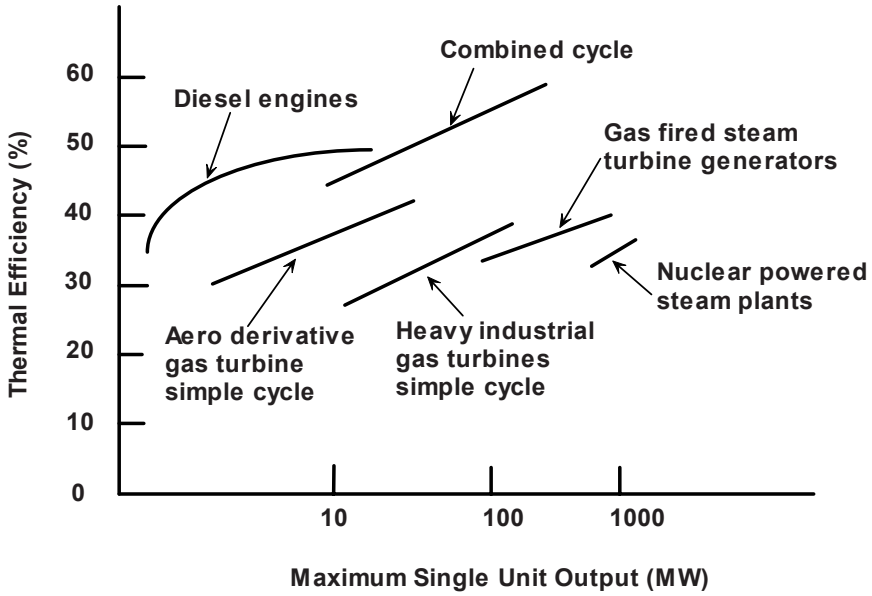

Fig. 4.24. Comparison of efficiency and power output of various power products [106].

Example 4.5

Consider a combined Brayton-Rankine cycle. The gas turbine of the Brayton cycle takes in air at 100 kPa and 25°C, has a pressure ratio of 5 and the temperature of the exhaust steam is 850°C. The gas turbine exhaust provides the energy input to the boiler of the Rankine cycle. The exhaust gas temperature from the boiler is 75°C. It may be assumed that the Rankine cycle is operating between 10 kPa and 4 MPa with a maximum temperature of 400°C. Assume that the total power output from the steam turbine is 100 MW. Calculate the efficiency of individual cycle, and that of the combined cycle.

Solution

First calculate the efficiency of the Rankine cycle

The *T-s* diagram of the combined cycle is shown in Fig. 4.23. The following values are obtained from the steam table.

h_1 (saturated liquid at 10 kPa) = 191.8 kJ/kg
$h_2 = h_1$ (neglecting work input to the pump) = 191.8 kJ/kg
h_3 (superheated steam, 400°C and 4 MPa) = 3214 kJ/kg
s_3 (superheated steam, 400°C and 4 MPa) = 6.7698 kJ/kg.

In State 4, both vapor and liquid exist. Therefore, we need to calculate the quality of the steam, x_4.

$$x_4 = \frac{s_4 - s_f}{s_{fg}} = \frac{7.7698 - 0.6491}{7.5019} = 0.8159$$

$$h_4 = h_f - x_4 h_{fg} = 191.8 + 0.8159 \times 2393 = 2144 \text{ kJ/kg}$$

Heat input to the boiler

$$q_B = h_3 - h_2 = 3214 - 191.8 = 3022.2 \text{ kJ/kg}$$

Work output by turbine

$$w_T = h_3 - h_4 = 3214 - 2144 = 1070 \text{ kJ/kg}$$

The thermal efficiency

$$\eta_{Rankine} = \frac{1070}{3022.2} = 0.3541 \text{, or } 35.41\%$$

The thermal efficiency of the Brayton cycle is given by

$$\eta_{Brayton} = 1 - r^{1-k/k} = 1 - (5)^{1-1.4/1.4} = 0.369 \text{ or } 36.9\%$$

Efficiency of the Combined Cycle

We need to calculate the power output from the gas turbine. In order to calculate this, mass flow rate of air to the gas turbine compressor should be calculated first.

Steam mass flux is calculated from the following expression.

$$\dot{w}_{Steam} = \dot{m}_s (h_3 - h_4); \quad 100\,000 = \dot{m}_s (3214 - 2144); \quad \dot{m}_s = 93.46 \text{ kg/s}$$

Temperatures at various location of the Brayton cycle are calculated next.

$$T_6 = T_5 \left(\frac{P_6}{P_5} \right)^{k-1/k} = (25 + 273)(5)^{\frac{1.4-1}{1.4}} = 472 \text{ K}$$

$$T_8 = T_7\left(\frac{P_8}{P_7}\right)^{k-1/k} = (850+273)\left(\frac{1}{5}\right)^{1.4-1/1.4} = 709\,\text{K}$$

Heat balance in the boiler provides

$$\dot{m}_s(h_3 - h_2) = \dot{m}_a C_p(T_8 - T_9)$$
$$93.46 \times (3214 - 191.8) = \dot{m}_a \times 1.0 \times [709 - (75+273)]$$

$$\dot{m}_a = 786\ \text{kg/s}$$

The output of the gas turbine is given by

$$\dot{W}_{gas\,turbine} = \dot{m}_a C_p(T_7 - T_8) = 786 * 1.0 \times (1123 - 709) = 325.5\ \text{MW}$$

The input work to compressor is:

$$\dot{W}_{compressor} = \dot{m}_a C_p(T_6 - T_5) = 136.9\ \text{MW}$$

The net output from the gas turbine,

$$\dot{W}_{Total} = \dot{W}_{gas\,turbine} - \dot{W}_{compressor} = 325.5 - 136.9 = 188.6\ \text{MW}$$

The energy input to the combustion chamber,

$$q_{in} = \dot{m}_a C_p(T_7 - T_6) = 786.5 \times 1.0 \times (1123 - 472) = 512\ \text{MW}$$

The efficiency of the combined cycle

$$\eta = \frac{100 + 188.6}{512} = 0.564\text{, or } 56.4\%$$

4.11 Stirling Cycle

The components of a Stirling cycle are shown in Fig. 4.25.

The Stirling cycle has several advantages when used in a Stirling engine, also known as the hot air engine. A Stirling engine is a heat engine. The heat-exchange process allows for near-ideal efficiency for conversion of heat into mechanical energy by following the Carnot cycle as closely as is practically possible with the given materials [107–111]. During the transfer stroke, the regenerator can rapidly transfer the heat to the working fluid reducing the amount of heat necessary from the external source. This has a positive effect on the thermal efficiency. Also, substitution of two isentropic processes with two constant volume processes results in increasing the work done as evident from the *P*-*v* diagram (Fig. 4.26). The *T*-*s* diagram is shown in Fig. 4.27.

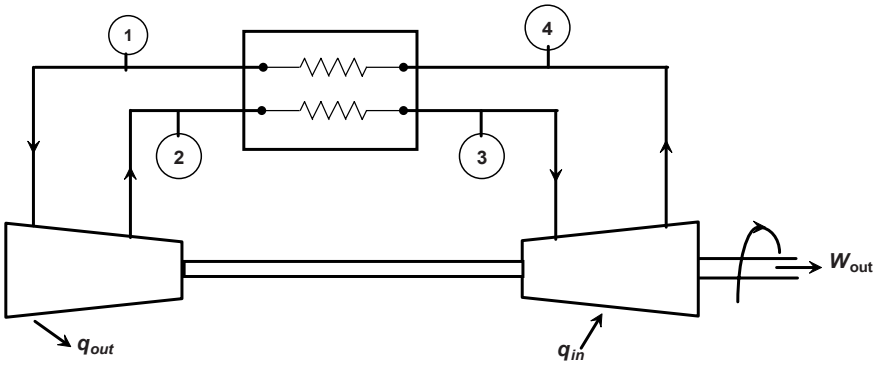

Fig. 4.25. Schematic diagram of a Stirling or Erricson Cycle.

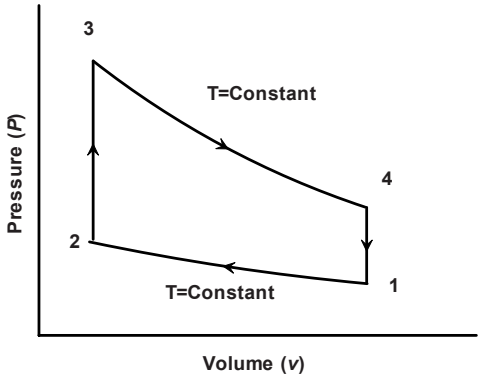

Fig. 4.26. *P*-*v* diagram of the Stirling cycle.

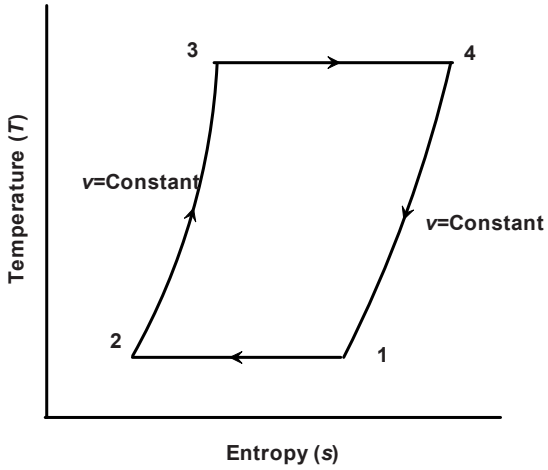

Fig. 4.27. *T-s* diagram of the Stirling cycle.

4.11.1 Efficiency of the Stirling Cycle

For an air-standard Stirling cycle, Kongtragool and Wongwises [112] derived an expression for calculating the thermal efficiency. The amounts of heat added and rejected per unit mass of working fluid can be expressed by the following expression [113]:

$$q_{in} = xC_v\left(T_H - T_C\right) + R\,T_H\,\ell n\frac{v_1}{v_2} \tag{4.49}$$

$$q_{out} = xC_v\left(T_C - T_H\right) + R\,T_C\,\ell n\frac{v_2}{v_1} \tag{4.50}$$

The parameter x is defined as the fractional deviation from the ideal regeneration ($x = 1$ for no regeneration and $x = 0$ for ideal regeneration), C_v is the specific heat capacity at constant volume in J/(kg K), T_H is the source temperature in the Stirling cycle in K, T_C is the sink temperature in K, R is the gas constant in J/(kg K), v_1 and v_2 are specific volumes of the constant-volume regeneration processes of the cycle in m^3/kg, and v_2/v_1 is the volume compression ratio. With these parameters, the Stirling cycle efficiency can be expressed as:

$$\eta_s = \frac{1 - T_C / T_H}{1 + \left(\frac{xc_v}{R\,\ell n \frac{v_1}{v_2}} \right) \left(1 - \frac{T_C}{T_H} \right)} \tag{4.51}$$

4.12 Ericssion Cycle

The Ericsson engine, which is based on the Ericsson cycle, is also known as an "external combustion engine", because it is externally heated [114–118]. To improve efficiency, the engine has a recuperator or regenerator between the compressor and the expander. The engine can be run either as an open cycle or as a closed cycle.

The Ericsson Cycle is often compared to the Stirling Cycle, since the engines based on these cycles are both external combustion engines with regenerators. Theoretically, both of these cycles have so called *ideal* efficiency, and it is estimated from the following expression:

$$\eta = 1 - \frac{T_C}{T_H} \tag{4.52}$$

The Ericsson Engine comprises of an air compressor that pumps air into a tank. The heat loss from the tank essentially maintains a constant temperature, thus approximating isothermal compression. From the tank, the compressed air passes through the regenerator and picks-up heat on the way to the heated power cylinder. The air is expanded in the cylinder at a constant temperature. Before the air is released as exhaust, it is passed back through the regenerator, thus heating the air for the next cycle. The *P-v* and *T-s* diagrams of the cycle are shown below in Figs. 4.28 and 4.29, respectively.

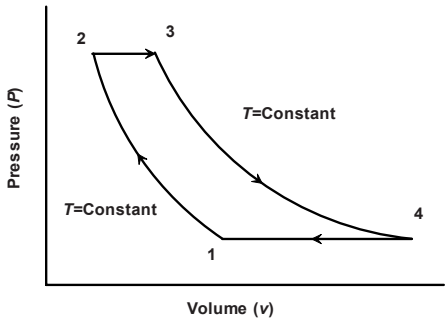

Fig. 4.28. *P-v* diagram of the Ericsson cycle.

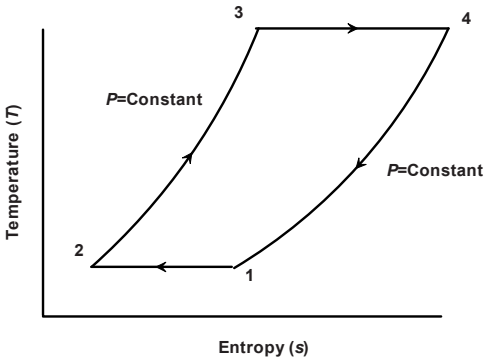

Fig. 4.29. *T-s* diagram of the Ericsson cycle.

4.13 Miller Cycle

Internal combustion engine based on Miller cycle was first used in ships and stationary power-generating plants, but recently was adapted by Mazda for their *KJ-ZEM*-V6, Millenia sedan. Subaru has also combined a Miller cycle flat-4 with a hybrid driveline for their "Turbo Parallel Hybrid" car, known as the Subaru *B5-TPH*.

Assuming constant specific heats, the efficiency of the Miller cycle can be expressed as

$$\eta = 1 - r^{(1-k)} \tag{4.53}$$

Miller [119] proposed a different Otto cycle with unequal compression and expansion strokes. The basic Miller cycle is very much like the Otto cycle that utilizes the four-stroke method. The difference is in the compression stroke. Figure 4.30 is the *P–v* diagram of the four-stroke Miller cycle without supercharger. In this figure, process 1–2 is an isobaric process; process 2–3 is an isobaric process if the intake valve is closed late; process 3–4 is an isentropic compression process; process 4–5 is an isochoric heating process; 5–6 is an isentropic expansion process; process 6–7 is an isochoric cooling process; and process 7–1 is an isobaric cooling process with the exhaust valve open.

Miller cycle efficiency may be enhanced by a number of methods [120, 121] including the use of a variable valve timing scheme during the combustion process [122]. Recently the emphasis is to reduce the emission from Miller engines by using a lean burn engine [123–129].

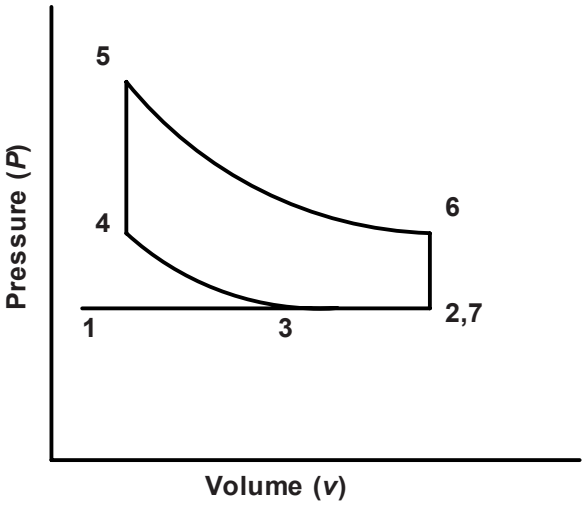

Fig. 4.30. The *P-v* diagram of a four-stroke Miller cycle (intake valve closed late).

4.14 Atkinson Cycle

The Atkinson cycle [130–136] is also refered to as a four stroke piston engine in which the intake valve is held open longer than normal to allow a reverse flow of intake air into the intake manifold. This modification resulted in improved fuel economy over the Otto cycle, because the compression ratio in a spark ignition engine is limited by the octane rating of the fuel used. The disadvantage of the four-stroke Atkinson cycle engine versus the more common Otto cycle engine is reduced power density. The Atkinson cycle is increasingly used in modern hybrid electric cars. The engine is only run at high powers intermittently, and the power of the engine is supplemented by an electric motor during times when high power is needed. This forms the basis of an Atkinson cycle based hybrid electric drive-train. Currently, Toyota's Prius and Camry, and Ford's Escape hybrid electric cars utilize Atkinson cycle.

The Atkinson cycle is internally reversible, but externally irreversible, since there is external irreversibility of heat transfer during the processes of constant volume heat addition and constant pressure heat rejection. The *T-s* diagram of the Atkinson cycle is shown in Fig. 4.31.

The Atkinson cycle starts with adiabatic compression of a vapor to an intermediate pressure and heating it at a constant volume to a high pressure P_3 at temperature T_3. Following this, an adiabatic expansion takes place to produce work from P_3 to P_4, and then cooling occurs at constant pressure P_4 to complete the cycle.

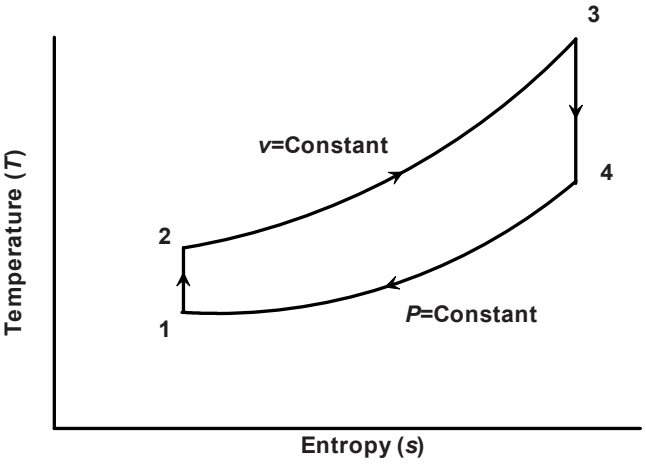

Fig. 4.31. The *T-s* diagram of the Atkinson cycle.

The thermal efficiency can be calculated from the following expression:

$$\eta = 1 - k\left(\frac{1}{r_c}\right)^{k-1} \frac{r-1}{\left(r^k - 1\right)} \tag{4.54}$$

where, r is the ratio of expansion ratio to compression ratio ($r = r_e/r_c$), r_c is compression ratio, and r_e is the expansion ratio and are given by the following expressions, respectively:

$$\begin{aligned} r_c &= \left(\frac{v_1}{v_2}\right) = \left(\frac{P_2}{P_1}\right)^{1/k} = \left(\frac{T_2}{T_1}\right)^{\frac{1}{k-1}} \\ r_e &= \left(\frac{v_4}{v_3}\right) = \left(\frac{P_3}{P_4}\right)^{1/k} = \left(\frac{T_3}{T_4}\right)^{\frac{1}{k-1}} \end{aligned} \tag{4.55}$$

4.15 Kalina Cycle

The Kalina cycle [137–154], which uses an ammonia-water mixture, has a higher energy efficiency than a conventional Rankine cycle by about 10–20%. The

increased efficiency resulted from the use of ammonia/water mixture as the working fluid, rather than the pure water or pure ammonia that is used in a standard Rankine cycle. The Kalina cycle is found to be more appropriate and efficient for use in Ocean Thermal Energy Conversion (OTEC) systems. For OTEC power systems, almost 80% increase in the efficiency over previous closed-cycle designs have been claimed. The Kalina cycle takes advantage of the variable boiling and condensing temperatures of ammonia/water mixtures.

The OTEC Kalina cycle uses the four typical Rankine cycle phases: evaporation, expansion, condensation and feed. An additional piece of equipment, the recuperator, recovers heat from the warm, but unvaporized, liquid leaving the separator vessel. A simplified schematic diagram of the system is shown in Fig. 4.32.

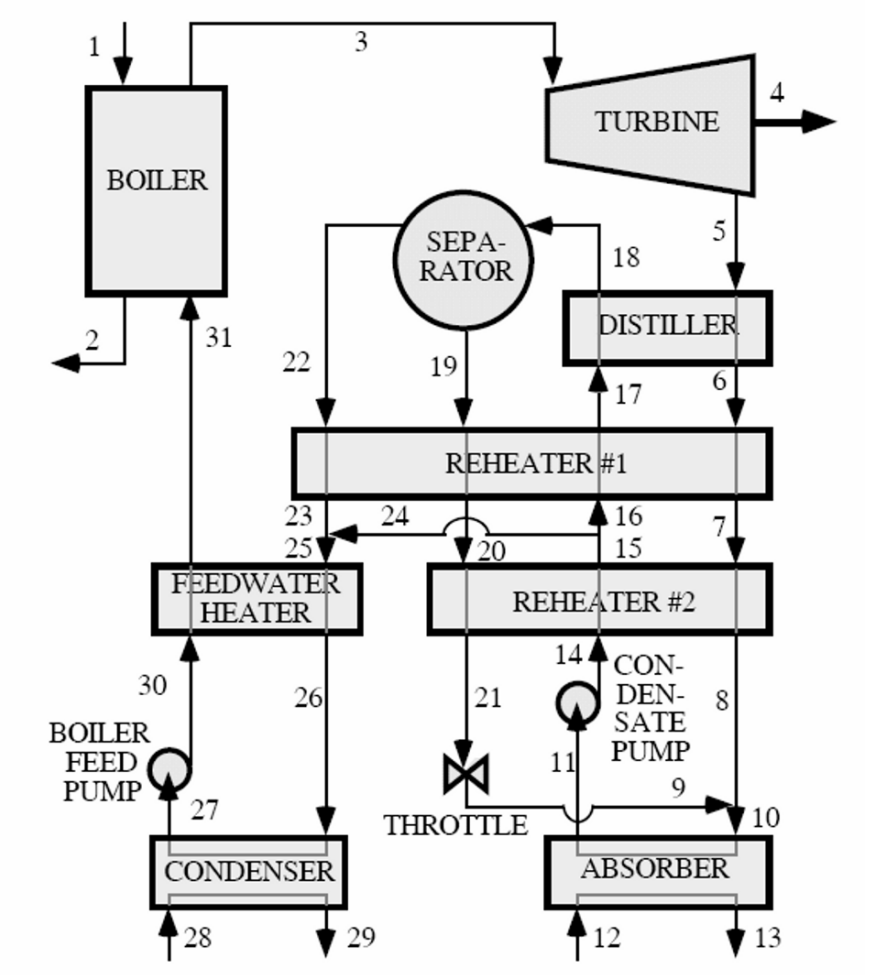

Fig. 4.32. The schematic diagram of a Kalina Cycle.

The Kalina cycle may be considered as a bottoming cycle feed, where the exhaust gases is fed to the boiler (1–2) to obtain superheated ammonia-water vapor (3), which is expanded in a turbine to generate work (4). The turbine exhaust (5) goes through a series of heat exchanger for cooling (6, 7, 8). The exhaust is diluted with ammonia-poor liquid (9, 10) and condensed (11) in the absorber by cooling water (12, 13). The saturated liquid leaving the absorber is compressed (14) to an intermediate pressure and heated (15, 16, 17, and 18). The saturated mixture is separated into an ammonia-poor liquid (19) which is cooled (20, 21) and depressurized in a throttle, and ammonia-rich vapor (22) is cooled (23) and some of the original condensate (24) is added to the nearly pure ammonia vapor to obtain an ammonia concentration of about 70% in the working fluid (25). The mixture is then cooled (26), condensed (27) by cooling water (28, 29), compressed (30), and sent to the boiler via regenerative feedwater heater (31). The *T-s* diagram of the cycle is shown in Fig. 4.33.

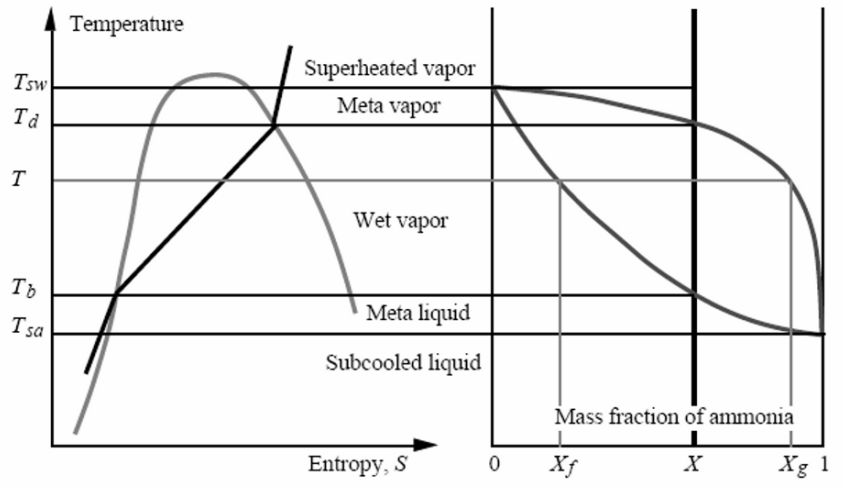

Fig. 4.33. The Kalina cycle in *T-s* diagram and corresponding thermodynamic state of ammonia-water mixture.

References

1. Zemansky MW (1968) Heat and Thermodynamics: An Intermediate Textbook. 5th ed. New York, McGraw-Hill
2. Van Ness HC (1983) Thermodynamics. Dover Publications, Inc.
3. Sonntag RE, Borgnakke C, Van Wylen GJ (1998) Fundamentals of Thermodynamics. 6th ed. New York, Wiley

4. Van Wylen GJ, Sonntag RE (1973) Fundamentals of Classical Thermodynamics. New York, Wiley
5. Schmidt PS, Ezekoye O, Howell JR, Baker D (2005) Thermodynamics: An Integrated Learning System. 1st ed. New York, Wiley
6. Shapiro M (2004) Fundamentals of Engineering Thermodynamics, 5th ed, New York, Wiley
7. Kaminski D, Jensen MK (2005) Introduction to Thermal and Fluid Engineering. New York, Wiley
8. Pulkrabek WW (1997) Engineering Fundamentals of the Internal Combustion Engine. New Jersey, Prentice Hall
9. Heywood JB (1997) Internal Combustion Engine Fundamentals. New York, McGraw-Hill
10. Curzon FL, Ahlborn B (1975) Efficiency of Carnot engine at maximum power output. Am J Phys 43: 22–24
11. Roco JMM, Velasco S, Medina A, Hernandez AC (1997) Optimum performance of a regenerative Brayton thermal cycle. Journal of Applied Physics 82(6): 2735–2741
12. Doty FD, Jones JD (1990) A new look at the closed Brayton cycle. Proceedings of the Intersociety Energy Conversion Engineering Conference 25th, 2: 166–172
13. Decher R (1987) Power density optimization of Brayton cycle engines. Proceedings of the Intersociety Energy Conversion Engineering Conference, 22: 1359–1363
14. Hiller CC (1979) Sensitivity study of Brayton cycle power plant performance. NTIS Report (1978), (SAND-78-8020), Energy Res. Abstr. 4(3), Abstr. No. 5518, 1979
15. Pietsch A (1969) Closed Brayton cycle power system applications, Proc. Intersoc. Energy Convers. Eng. Conf 4th, pp. 642–651
16. Stewart WL (1967) Brayton cycle technology, NASA (Nat. Aeronaut. Space Admin.), Access. (1966), (NASA-SP-131), pp. 95–145. From: Sci. Tech. Aerospace Rept. 5(1), N67-10266, 1967
17. Chen L, Ni N, Cheng G, Sun F, Wu C (1999) Performance analysis for a real closed regenerated Brayton cycle via methods of finite-time thermodynamics. International Journal of Ambient Energy 20(2): 95–104
18. Brokaw RS (1961) Thermal conductivity and chemical kinetics. Journal of Chemical Kinetics 35, 1569–1580
19. Schleicher R, Raffray AR, Wong CP (2001) An assessment of the Brayton cycle for high performance power plants. Fusion Technology, 39(2, Pt. 2): 823–827
20. Negri di Montenegro G, Bettocchi R, Cantore G, Borghi M, Naldi G (1988) A comparative study on the ways of converting steam power plants to steam-gas combined cycle power plants. Ist. Macch Proceedings of the Intersociety Energy Conversion Engineering Conference, 23rd 1: 301–306
21. Schwarz N (1984) Increasing the efficiency of thermal power stations, Oesterr. Forschungszent. Seibersdorf, [Ber.] OEFZS (OEFZS BER. No. 4261), 20 pp
22. Krasin K and Nesterenko V. B (1971) Dissociating gases: a new class of coolants and working substances for large power plants, Atomic Energy Review, 9, 177–194
23. Peterson PF (2003) Multiple-reheat Brayton cycles for nuclear power conversion with molten coolants. Nuclear Technology 144(3): 279–288
24. Fenech H, Saunders RJ (1989) Application of heat storage reservoirs to improve the performance of Brayton cycle nuclear power plants with atmospheric heat rejection. Annals of Nuclear Energy 16(4): 203–209

25. Walter A (2006) System modeling and simulation of HTR circuits with Brayton cycle for operational and accidental conditions. Wissenschaftliche Berichte - Forschungszentrum Karlsruhe (FZKA 7155), pp. 181–186.
26. Walter A, Alexander S, Guenter L (2006) Comparison of two models for a pebble bed modular reactor core coupled to a Brayton cycle. Nuclear Engineering and Design 236(5–6): 603–614
27. Frye PE, Robert A, Rex D (2005) Brayton power conversion system study to advance technology readiness for nuclear electric propulsion - phase I. AIP Conference Proceedings (2005), 746 (Space Technology and Applications International Forum–STAIF 2005), pp. 727–737
28. Wang J, Gu Y (2005) Parametric studies on different gas turbine cycles for a high temperature gas-cooled reactor. Nuclear Engineering and Design 235(16): 1761–1772
29. Wang H, Wang C (2005) A closed cycle helium gas turbine plant used for a high-temperature gas cooled reactor-based electric power generation unit. Reneng Dongli Gongcheng 20(4): 337–341
30. Lipinski RJ, Wright SA, Dorsey DJ, Peters CD, Brown N, Williamson J, Jablonski J (2005) A gas-cooled-reactor closed- Brayton – cycle demonstration with nuclear heating. AIP Conference Proceedings 746 (Space Technology and Applications International Forum--STAIF 2005): 437–448
31. Chaudourne S (1990) Optimization of a heat pipe radiator for a 20-kWe Brayton cycle space power system. Proc. Symp. Space Nucl. Power Syst 7th 2: 633–638
32. Tilliette ZP, Proust E, Carre F (1987) Progress in investigating Brayton cycle conversion systems for future French Ariane 5 space power applications. Proceedings of the Intersociety Energy Conversion Engineering Conference (1987), 22nd 1: 438–443
33. Barrett MJ, Johnson PK (2005) Performance and mass modeling subtleties in closed-Brayton – cyclespace power systems. NASA/TM (2005), (2005-213985), i, 1–12
34. Barrett MJ, Reid BM (2004) System mass variation and entropy generation in 100-kWe closed- Brayton – cycle space power systems. NASA/TM (2004), (NASA/TM-2004-212741): 1–8
35. El-Genk, MS, Tournier, J-M (2006) High temperature water heat pipes radiator for a Brayton space reactor power system. AIP Conference Proceedings (2006), 813(Space Technology and Applications International Forum–STAIF 2006): 716–729
36. Joyner CR II, Fowler B, Matthews J (2003) A closed Brayton power conversion unit concept for nuclear electric propulsion for deep space missions. AIP Conference Proceedings (2003), 654(Space Technology and Applications International Forum–STAIF 2003): 677–684
37. Stasa FL, Osterle F (1981) The thermodynamic performance of two combined cycle power plants integrated with two coal gasification systems. Journal of Engineering for Power 103(3): 572–581
38. Iles TL, Ruder JM (1982) Brayton cycle waste heat recovery system. Proc Int Gas Res Conf 2nd: 1069–1080
39. Amann CA (1999) Evaluating alternative internal combustion engines: 1950–1975, Journal of Engineering for Gas Turbines and Power, 121: 540–545
40. Rogers C, McDonald CF (1997) Automotive turbogenerator design considerations and technology evolution, Society of Automotive Engineers. Technical Paper 972673.11, 1997
41. Wilson DG (1997) A New approach to low-cost high efficiency automotive gas turbines, society of automotive engineers. Technical Paper 970234

42. Wilson DG (1978) Alternative automobile engines, Scientific American, 239(1): 39–49
43. McDonald F, Etzel K.T (1995) The closed Brayton cycle - a fuel neutral gas turbine to meet energy user's needs in the Pacific Rim nations. Proceedings of the American Power Conference 57(1): 382–387
44. Mason JL (1967) Working gas selection for the closed Brayton cycle, AGARDograph, Volume Date 1964(81): 223–252
45. Kesavan K, Osterle JF (1982) Split-flow nuclear gas turbine cycle using dissociating N_2O_4, Paper 82–GT–181, The American Society of Mechanical Engineers, New York
46. Krasin K (1975) Dissociating Gases as Heat-Transfer Media and Working Fluids in Power Installations, AEC-tr-7295, translated and published for the Atomic Energy Commission and the National Science Foundation by Amerind Publishing, New Delhi
47. Lighthill MJ (1957) Dynamics of a dissociating gas Part I equilibrium flow. Journal of Fluid Mechanics 2: 1–32
48. Stochl RJ (1979) Potential performance improvement using a reacting gas (Nitrogen Tetroxide) as the working fluid in a closed Brayton cycle, NASA TM–79322
49. Dostal V, Hejzlar P, Driscoll MJ (2006) The supercritical carbon dioxide power cycle: comparison to other advanced power cycles. Nuclear Technology 154(3): 283–301
50. Dostal V, Hejzlar P, Driscoll MJ (2006) High-performance supercritical carbon dioxide cycle for next-generation nuclear reactors. Nuclear Technology 154(3): 265–282
51. Sahin B, Kodal A, Yavuz H (1995) Efficiency of a Joule–Brayton engine at maximum power density. Journal of Physics Series D: Applied Physics 28: 1309–1313
52. Wu C, Chen L, Sun F (1996) Performance of regenerative Brayton heat engines. Energy International Journal 21(2): 71–76
53. Cheng CY, Chen CK (1997) Ecological optimization of an irreversible Carnot heat engine. Journal of Physics Series D: Applied Physics 30: 1602–1609
54. Cheng CY, Chen CK (1998) Ecological optimization of an endoreversible Brayton cycle. Energy Conversion and Management 39: 33–44
55. Wu C, Chen L, Chen J (1999) Recent Advances in Finite-Time Thermodynamics. New York, Nova Science
56. Chen L, Zheng J, Sun F, Wu C (2001) Power density optimization for an irreversible regenerated closed variable temperature heat reservoir Brayton cycle. Journal of Physics Series D: Applied Physics 34(11): 1727–1739
57. Chen L, Zheng J, Sun F, Wu FC (2001) Power density analysis and optimization of a regenerated closed Brayton cycle. Physica Scripta 64(3): 184–191
58. Chen L, Zheng J, Sun F, Wu C (2002) Performance comparison of an endoreversible closed variable temperature heat reservoir Brayton cycle under maximum power density and maximum power conditions. Energy Conversion and Management 43:33–43.
59. Akash BA (2001) Effect of heat transfer on the performance of an air-standard diesel cycle. International Communications in Heat and Mass Transfer 28(1): 87–95
60. Pirouzpanah V, Kashani BO (1999) A diesel engine cycle model for prediction of performance and pollutants emission, in Energy and the Environment, Editor(s): I. Dincer and T. Ayhan, Proceedings of the Trabzon International Energy and Environment Symposium, 2nd, Trabzon, Turkey, July 26–29: 101–105
61. Harris WD (1997) An external combustion, open-diesel cycle heat engine. Proceedings of the Intersociety Energy Conversion Engineering Conference, 32nd: 967–972
62. Blank DA, Wu C (1993) The effect of combustion on a power optimized endoreversible diesel cycle. Energy Conversion and Management 34(6): 493–498

63. Klein SA (1991) An explanation for observed compression ratios in internal combustion engines. Journal of Engineering for Gas Turbines and Power 113(4): 511–513
64. Hellen G (1994) Controlling NOx emissions at diesel power plants. Proceedings of the Institution of Mechanical Engineers, IMechE Conference (7): 107–112
65. Melton RB Jr, Lestz SJ, Quillian RD Jr, Rambie EJ (1975) Direct water injection cooling for military engines and effects on the diesel cycle. Symposium (International) on Combustion, Proceedings, 15: 1389–1399
66. Wang Y, Zeng S, Huang J, He Y, Huang X, Lin L, Li S (2005) Experimental investigation of applying Miller cycle to reduce NOx emission from diesel engine, Proceedings of the Institution of Mechanical Engineers, Part A: Journal of Power and Energy 219(A8): 631–638
67. Chen L, Ge Y, Sun F. Wu C (2006) Effects of heat transfer, friction and variable specific heats of working fluid on performance of an irreversible dual cycle. Energy Conversion and Management 47(18–19): 3224–3234
68. Zheng T, Chen L, Sun F, Wu C (2004) Finite time thermodynamic performance for an irreversible Dual cycle. Advances in Finite Time Thermodynamics: 51–61
69. Kokubu (1998) Development of dual fluid cycle gas turbine. Proceedings of the International Gas Research Conference, 5: 804–816
70. Juneja MN, Biswas DK, Majumder A, Singh S (1978) Coal gasification for dual cycle power generation. Chemical Engineering World 13(3): 45–49
71. Elliott VA, Trocki T (1957) Power conversion systems for dual-cycle boiling reactor. Selected Papers 1st Nuclear Eng. Sci. Congr, Cleveland, 1955, 1: 285–291
72. Untermyer S (1955) Dual cycle improves boiling-water reactors. Nucleonics 13(7): 34–35
73. Mandl F (1989) Statistical Physics, 2nd ed, Chichester, England, Wiley, pp. 121–123
74. Anderson HL (Ed.-in-Chief) (1989) A Physicist's Desk Reference, American Institute of Physics, New York.
75. Ge Y, Chen L, Sun F, and Wu C (2005) Thermodynamic simulation of performance of an Otto cycle with heat transfer and variable specific heats of working fluid. International Journal of Thermal Sciences 44(5): 506–511
76. Vinokurov VA, Kaminskii VA, Frost VA, Kolesnikov IM (2000) Modeling of combustion processes in internal combustion engines. Chemistry and Technology of Fuels and Oils (Translation of Khimiya i Tekhnologiya Topliv i Masel) 36(6): 408–415
77. Boggs DL, Hilbert HS, Schechter MM (1995) The Otto-Atkinson cycle engine-fuel economy and emissions results and hardware design. Society of Automotive Engineers, [Special Publication] SP, SP-1108 (Futuristic Concepts in Engines and Components): 47–59
78. Angulo-Brown F, Rocha-Martinez JA, and Navarrete-Gonzalez TD (1996) A non-endoreversible Otto cycle model: improving power output and efficiency. Journal of Physics D: Applied Physics 29(1): 80–83
79. Klimstra J, Bijma BJ, Westing JE (1993) Efficiency determination of turbochargers for Otto-cycle engines. Society of Automotive Engineers, [Special Publication] SP, SP-993 (Gaseous Fuel Technology For The Nineties): 43–55
80. Rakopoulos CD (1993) Evaluation of a spark ignition engine cycle using first and second law analysis techniques. Energy Conversion and Management 34(12): 1299–1314
81. Wu C, Blank DA (1993) Optimization of the endoreversible Otto cycle with respect to both power and mean effective pressure. Energy Conversion and Management 34(12) 1315–1318

82. Wu C, Blank DA (1992) The effects of combustion on work-optimized endo-reversible Otto cycle. Journal of the Institute of Energy 65(463): 86–89
83. Maly R (1990) Improved Otto cycle by enhancing the final phase of combustion, Comm. Eur. Communities, [Rep.] EUR (EUR 12467)
84. Patrick RS (1989) Air-fuel ratio estimation in an Otto cycle engine: two methods and their performance, Ph.D. Dissertation, Stanford University, Stanford, CA, USA
85. Lior N, Rudy GJ (1988) Second-law analysis of an ideal Otto cycle. Energy Conversion and Management 28(4): 327–334
86. Brown GG (1938) A thermodynamic analysis of the rate of rise of pressure in the Otto cycle. Chemical Reviews 22: 27–49
87. Rosecrans CZ, Felbeck GT (1925) A thermodynamic analysis of gas engine tests. Univ. Ill. Eng. Expt. Sta, Bull.150
88. Eldighidy SM (1993) Optimum outlet temperature of solar collector for maximum work output for an Otto air-standard cycle with ideal regeneration. Solar Energy 51(3): 175–182
89. Lee WY, Kim SS (1991) Analytical formula for the estimation of a Rankine-cycle heat engine efficiency at maximum power. International Journal of Energy Research 15: 149–159
90. Bejan A (1988) Advanced Engineering Thermodynamics. New York, Wiley
91. El-Wakil MM (1984) Powerplant Technology, New York, McGraw-Hill
92. Wood BD (1969) Applications of Thermodynamics. Reading, MA, Addison-Wesley
93. Bernard DW (1969) Application of Thermodynamics. Reading, MA, Addison-Wesley
94. Kern T.-U, Wieghardt K., Kirchner H (2005) Material and design solutions for advanced steam power plants. Advances in Materials Technology for Fossil Power Plants, Proceedings from the International Conference, 4th, Hilton Head Island, SC, United States, Oct. 25–28, 2004 Meeting Date 2004: 20–34
95. Ellis FV, Wright IG, Maziasz PJ (2005) Review of turbine materials for use in ultra - supercritical steam cycles. Advances in Materials Technology for Fossil Power Plants, Proceedings from the International Conference, 4th, Hilton Head Island, SC, United States, Oct. 25–28, 2004 Meeting Date 2004: 535–551
96. Macmillan JH (1965) Nuclear power and supercritical steam cycles. Proceedings of the American Power Conference 27: 243–247
97. Potter JH (1969) Totally supercritical steam cycle. Journal of Engineering for Power 91(2): 113–120
98. Szewalski R (1974) New high-efficiency steam power cycle for supercritical steam conditions. Prace Instytutu Maszyn Przeplywowych, Polska Akademia Nauk 64: 3–20.
99. Sedler B (1975) Application of a regenerative heat exchanger for supercritical parameters in steam and water cycle of a steam power plant. Prace Instytutu Maszyn Przeplywowych, Polska Akademia Nauk 66: 29–43
100. Reuter FD (1993) Steam generator for power plant concepts with high efficiency. VDI-Berichte 1029: 124–140
101. Miyashita K (1997) Overview of advanced steam plant development in Japan. IMechE Conference Transactions (2, Advanced Steam Plant): 17–30
102. Swanekamp R (2001) Supercritical steam cycle delivers efficient and reliable performance. Power 145(4): 87–88
103. De S, Nag PK (2000) Thermodynamic analysis of a partial gasification pressurized combustion and supercritical steam combined cycle. Proceedings of the Institution of Mechanical Engineers, Part A: Journal of Power and Energy 214(A6): 565–574

104. Dostal V, Hejzlar P, Todreas NE, Buongiorno J (2004) Medium-power lead-alloy fast reactor balance-of-plant options. Nuclear Technology 147(3): 388–405
105. Tsiklauri G, Talbert R, Schmitt B, Filippov G, Bogoyavlensky R, Grishanin E (2005) Supercritical steam cycle for nuclear power plant. Nuclear Engineering and Design 235(15): 1651–1664
106. Dominic B (1997) Comparison of efficiency and power output of various power products, Keynote talk, 1997 International Gas Turbine Institute (IGTI) Turbo Expo
107. Simon TW, Seume JR (1990) The Stirling engine: an engine that requires high-flux heat exchange under oscillating flow conditions, In: R. K. Shah, A. D. Kraus, and D. Metzger (Eds), Compact Heat Exchangers. New York, Hemisphere Publishing, pp. 567–626
108. Walker G (1980) Stirling Engines. Oxford, Clarendon Press
109. West CD (1986) Principles and Applications of Stirling Engines. New York, Van Nostrand Rheinhold
110. Allan J (1992) Thermodynamics and Gas Dynamics of the Stirling Cycle Machine. Cambridge, Cambridge University Press
111. Urieli, A, Berchowitz DM (1984) Stirling Cycle Engine Analysis. Bristol, Adam Higler Ltd.
112. Kongtragool B, Wongwises S (2003) A review of solar-powered stirling engines and low temperature differential Stirling engines. Renewable and Sustainable Energy Reviews 7: 131–154
113. Howell JR, Bannerot RB (1977) Optimum solar collector operation for maximizing cycle work output. Solar Energy 19: 149–153
114. Erbay LB, Sisman A, Yavuz H (1996) Analysis of Ericsson cycle at maximum power density conditions. ECOS'96, Stockholm, June 25–27: 175–178
115. Cataldo RS (1979) Modified Ericsson cycle engine, US Patent 4133172
116. Corey JA (1991) Ericsson cycle machine, US Patent 4984432
117. Blank DA, Chih W (1996) Power limit of an endoreversible Ericsson cycle with regeneration. Energy Conversion and Management, 37(1): 59–66(8)
118. Berrin L, Sisman A, and Yavuz H (1996) Analysis of Ericsson cycle at maximum power density conditions. ECOS: 25–27
119. Miller RH (1947) Supercharging and internally cooling for high output. ASME Transactions 69: 453–464
120. Al-Sarkhi J, Jaber O, Probert SD (2006) Efficiency of a Miller engine. Applied Energy 83(4): 343–351
121. Ge Y, Chen L, Sun F, Wu C (2005) Effects of heat transfer and friction on the performance of an irreversible air-standard Miller cycle. International Communications in Heat and Mass Transfer 32(8): 1045–1056
122. Fontana G, Galloni E, Palmaccio R, Torella E (2006) The influence of variable valve timing on the combustion process of a small spark-ignition engine. Proceedings of Automotive Engineers, [Special Publication] SP, SP-2011(Multi-Dimensional Engine Modeling 2006): 151–160
123. Kesgin U (2005) Efficiency improvement and NOx emission reduction potentials of two-stage turbocharged Miller cycle for stationary natural gas engines. International Journal of Energy Research 29(3): 189–216
124. Shimoda H, Kakuhama Y, Noguchi T, Endo H, Tanaka K (2004) High efficiency miller cycle gas engine generator with clean and low carbon dioxide emission. Mitsubishi Juko Giho 41(1): 24–25

125. Kakuta A, Shimoda H, Takaishi T (2003) Mitsubishi lean-burn gas engine of the highest thermal efficiency in the world. Mitsubishi Juko Giho 40(4): 246–249
126. Fujiwaka T, Kakuhama Y (2001) Development of lean burn Miller cycle gas engine. Proceedings of the International Gas Research Conference RCP31/1-RCP31/14
127. Tsukida N, Abe T, Okamoto K, Takemoto T (1999) Development of Miller cycle gas engine for cogeneration. AES (American Society of Mechanical Engineers) 39(Proceedings of the ASME Advanced Energy Systems Division–1999): 453–457
128. Fujiwaka T, Tsurusaki M, Shimoda H, Endo H (1998) Development of the Miller cycle lean burn gas engine. Proceedings of the International Gas Research Conference, 4: 336–345
129. Okamoto K, Zhang F-R, Shimogata S, and Shoji F (1997) Development of a late intake-valve closing (LIVC) Miller cycle for stationary natural gas engines - effect of EGR utilization. Society of Automotive Engineers, [Special Publication] SP, SP-1305(Preparing Mixtures for Diesel and SI Engines): 87–99
130. Bussing T, Pappas G (1994) An Introduction to Pulse Detonation Engines. Paper AIAA 94-0263, The American Institute of Aeronautics and Astronautics, Washington, D.C
131. Heywood JB (1988) Internal Combustion Engine Fundamentals. New York, McGraw-Hill
132. Kailasanath K, Patrick G, Li C (1999) Computational Studies of Pulse Detonation Engines – A Status Report. Paper AIAA 99-2634, The American Institute of Aeronautics and Astronautics, Washington, D.C
133. Wilson DG, Korakianitis T (1998) The Design of High-Efficiency Turbomachinery and Gas Turbines, 2nd ed. New Jersey, Prentice-Hall
134. Wilson MW (1999) Efficiency enhanced turbine engine. U. S. Patent Number 5966927, October 19
135. Chen L, Lin J, Sun F, Wu C (1998) Efficiency of an Atkinson engine at maximum power density. Energy Conversion and Management 39(3/4): 337
136. Wang P-Y, Hou S-S (2005) Performance analysis and comparison of an Atkinson cycle coupled to variable temperature heat reservoirs under maximum power and maximum power density conditions. Energy Conversion and Management 46: 2637–2655
137. Amano Y, Kawanishi K, Hashizume T (2005) Experimental investigations of oscillatory fluctuation in an ammonia-water mixture turbine system, AES (American Society of Mechanical Engineers), 45(Proceedings of the ASME Advanced Energy Systems Division–2005): 391–398
138. Prisyazhniuk VA, Holon I (2006) Strategies for emission reduction from thermal power plants. Journal of Environmental Management 80(1): 75–82
139. Borgert JA Velasquez JA (2004) Exergoeconomic optimisation of a Kalina cycle for power generation, International Journal of Energy 1(1): 18–28
140. Jonsson M (2003) Advanced power cycles with mixtures as the working fluid, PhD Dissertation, Kungliga Tekniska Hogskolan, Stockholm, Sweden
141. DiPippo R (2004) Second Law assessment of binary plants generating power from low-temperature geothermal fluids. Geothermics 33(5): 565–586
142. Bisio G, Rubatto G (2001) Marangoni effects and heat transfer variations in steam condensation by employing Kalina cycles. Proceedings of the Intersociety Energy Conversion Engineering Conference, 36th 2: 1171–1176

143. Dejfors C, Thorin E, and Svedberg G (1998) Ammonia-water power cycles for direct-fired cogeneration applications. Energy Conversion and Management 39(16–18): 1675–1681
144. Mlcak HA (1996) An introduction to the Kalina cycle, PWR (American Society of Mechanical Engineers), 30(Proceedings of the International Joint Power Generation Conference, 2: 765–776
145. Nag PK, Gupta AVSSKS (1998) Energy analysis of the Kalina cycle. Thermal Engineering 18(6): 427–439
146. Enick RM, Donahey GP, Holsinger M (1998) Modeling the high-pressure ammonia-water system with WATAM and the Peng-Robinson equation of state for Kalina cycle studies. Industrial & Engineering Chemistry Research 37(5): 1644–1650
147. Enick RM, Gale T, Klara J (1997) Modeling the application of Kalina cycle to LEBS power plants. Proceedings of the International Technical Conference on Coal Utilization & Fuel Systems, 22: 209–220
148. Rogdakis ED (1996) Thermodynamic analysis, parametric study and optimum operation of the Kalina cycle. International Journal of Energy Research, 20(4): 359–370
149. Marston CH, Sanyal Y (1994) Optimization of Kalina cycles for geothermal application, AES (American Society of Mechanical Engineers), 33 (Thermodynamics and the Design, Analysis, and Improvement of Energy Systems 1994): 97–104
150. Lazzeri L, Diotti F, Bruzzone M, Scala M (1995) Applications of Kalina cycle to geothermal applications. Proceedings of the American Power Conference 57(1): 370–373
151. Marston CH, Hyre M (1995) Gas turbine bottoming cycles: triple-pressure steam versus Kalina. Journal of Engineering for Gas Turbines and Power 117(1): 10–15
152. Kalina A, Leibowitz HM (994) Applying Kalina cycle technology to high-enthalpy geothermal resources. Transactions - Geothermal Resources Council, 18, Restructuring the Geothermal Industry: 531–536
153. Rumminger MD, Dibble RW, Lutz AE, Yoshimura AS (1994) An integrated analysis of Kalina cycle in combined cycles. Proceedings of the Intersociety Energy Conversion Engineering Conference, 29TH(PT.2), 974–979
154. Ibrahim MB, Kovach RM (1993) A Kalina cycle application for power generation. Energy (Oxford, United Kingdom) 18(9): 961–969

Problems

1. Steam enters the turbine of a power plant operating on the Rankine cycle at 3,300 kPa and leaves at 50 kPa. Determine the thermal efficiency of the cycle and the quality of the exhaust stream from the turbine for turbine-inlet stream temperatures of:
   (a) 475°C; (b) 550°C; and (c) 600°C.

   What effect will an increase in the turbine inlet stream temperature have on the following?

   (i) The thermal efficiency and
   (ii) The quality of the exhaust stream exiting the turbine

   If the turbine had an efficiency of 0.80, determine its impact on the thermal efficiency of the process at your temperature and its effect on the sizing of the equipment (the boiler, condenser, etc.).

2. Electrical power is to be produced from a steam turbine connected to a nuclear reactor. Steam is obtained from the reactor at 800 ºF and 700 psia and exits a turbine at 50 psia. The turbine operates adiabatically. Compute the maximum work per pound of steam that can be obtained from the turbine. Also show the process in a *P-v* and a *T-s* diagram.
   Note: use steam tables.
3. Electrical power is to be produced from a steam turbine connected to a nuclear reactor. Steam can be obtained from the reactor at 500 ºF and 600 psia and exits the turbine at 20 psia. The turbine operates adiabatically. Compute the maximum work per pound of steam that can be obtained from the turbine.

   Assume that the single turbine considered above is replaced by two adiabatic turbines with a reheat loop. In this modified process, the steam exiting from the first turbine is returned to the reactor, where it is reheated at constant pressure to 500 ºF, and then fed to the second stage of the turbine. Draw a process flow sheet for this suggested operation with labeled streams, where P' is the pressure for the stream exiting the first turbine.

   (a) Determine the maximum work obtained per pound of steam if the two turbine process is used and the exhaust pressure from the first turbine is P' = 310 psia.
   (b) Compute the maximum work obtained per pound of steam if the two turbine process is used and the exhaust pressure from the first turbine is P' = 35 psia.
   (c) Compute the heat adsorbed per pound of steam in the reheating steps in parts (a) and (b).
   (d) Show the process in a P-v and a T-s diagram.
   Note: use steam tables.

4. Consider the following air-standard thermodynamic cycle. Assume all processes are quasi-static and air behaves as an ideal gas.
   Air undergoes a quasi-static thermodynamic cycle 1–2–3–4–1 as shown above. Various conditions are given in the figure. The conditions at state 1 are p_1 = 100 kPa, T_1=300 K. The pressure ratio (p_2/p_1) over process 1–2 is 10 and the peak temperature of the cycle is 1,500 K. Assume that c_p = 1.0035 kJ/kg-K and c_v = 0.7165 kJ/kg-K are constants, and that R = 0.287 kJ/kg-K.

   (a) For each section of the cycle determine the heat flow, whether the heat added to the system, q_{in}, and the work done by the system, W_{in} and W_{out}.
   (b) For each section of the cycle calculate the work and heat transfer, the change in internal energy and the change in enthalpy.
   (c) What is the net work of the cycle?
   (d) What is the thermal efficiency of the cycle?

5. A Carnot heat engine produces power of 2.5 kW. It rejects heat to a river that is flowing at 2 kg/s, resulting in a temperature increase of 2°C. The average temperature of the river is 20°C. Determine

   (a) The heat transfer input required for the heat engine
   (b) The efficiency of the heat engine
   (c) The temperature at which heat transfer occurs to the engine

6. A device has an inlet flow of air at 20°C, 300 kPa, and 5 kg/s and two outlet flows, air at 60°C, 270 kPa, and 2 kg/s and air at 0°C, 270 kPa, and 3 kg/s. Verify if there is no work or heat transfer under these conditioned.

7. Determine the power output of an adiabatic turbine with isentropic efficiency 0.83 that has a steam input of 15 MPa and 650°C and an outlet pressure of 50 kPa.
8. Consider a steam power plant operating on a Rankine cycle with two open feedwater heaters. Steam leaves the boiler at 20 MPa and 670°C. The first high pressure open feedwater heater operates at 4 MPa, the low pressure open feedwater heater operates at 0.4 MPa, and the condenser operates at 0.004 MPa. Determine:
   (a) thermal efficiency of the plant
   (b) mass flow rate of steam leaving the boiler required to produce 60 MW of power.
9. Consider an internal combustion engine operating on the ideal Dual cycle with the following conditions: Two cylinder, four stroke engine with displacement of 1.6 l; Compression ratio of 7.5; Cutoff Ratio of 1.7; Combustion temperature of 1,700 K; Engine speed of 1,300 rpm. The initial temperature and pressure are taken to be 150 kPa and 315 K due to turbocharging of the intake air. Just before the final process (constant volume cooling) 85% of the air is extracted and is used to power a turbine that supplies power to the intake compressor (i.e. the turbocharger). Determine:
   (a) Engine thermal efficiency
   (b) Engine power output
   (c) Engine MEP
   (d) Exhaust turbine power